12-2016

A Portable and Automatic Biosensing Instrument for Detection of Foodborne Pathogenic Bacteria in Food Samples

Zhuo Zhao
University of Arkansas, Fayetteville

A Portable and Automatic Biosensing Instrument for Detection of Foodborne Pathogenic Bacteria in Food Samples

A thesis submitted in partial fulfilment
of the requirements for the degree of
Master of Science in Biological Engineering

by

Zhuo Zhao
China Agricultural University
Bachelor of Engineering in Automation, 2014

December 2016
University of Arkansas

This thesis is approved for recommendation to the Graduate Council.

Dr. Yanbin Li
Thesis Director

Dr. Yi Liang
Committee Member

Dr. Franck Carbonero
Committee Member

Abstract

Foodborne diseases are a growing public health problem. In recent years, many rapid detection methods have been reported, but most of them are still in lab research and not practical for use in the field. In this study, a portable and automatic biosensing instrument was designed and constructed for separation and detection of target pathogens in food samples using nanobead-based magnetic separation and quantum dots (QDs)-labeled fluorescence measurement. The instrument consisted of a laptop with LabVIEW software, a data acquisition card (DAQ), a fluorescent detector, micro-pumps, stepper motors, and 3D printed tube holders. First, a sample in a syringe was mixed with magnetic nanobead-antibody (MNB-Ab) conjugates and then injected to a low binding reaction tube. After incubation and magnetic separation, target bacterial cells were captured and collected and the solution was pumped out. Then the QD-antibody (QD-Ab) conjugates were pumped into the reaction tube to form the MNB-Ab-cell-Ab-QD complexes that were then collected by magnetic separation and resuspended in PBS buffer solution through air pressure control. Finally, the sample solution was pushed into the detection tube by an air pump and the fluorescence intensity was measured using a fluorescent detector. A virtual instrument (VI) was programmed using LabVIEW software to provide a platform for magnetic separation, fluorescent measurement, data processing, and control. The DAQ was used for data communication. The results showed that the separation efficiency of this instrument was 78.3 ± 3.4% and 60.7 ± 4.2% for *E. coli* O157:H7 in pure culture and ground beef samples, respectively. The limit of detection was 3.98×10^3 and 6.46×10^4 CFU/mL in pure culture and ground beef samples, respectively. Sample preparation and detection could be finished in 2 hours. The instrument was portable and automatic with great potential to serve as a more effective tool for in-field/on-line detection of foodborne pathogenic bacteria in food products.

Keywords. biosensor, automatic system, fluorescent detection, magnetic separation, foodborne pathogens

Acknowledgements

I would like to sincerely thank my advisor, Dr. Yanbin Li, for his help and support during my entire graduate program. I learned how to become a better researcher with his informative and constructive advice. He not only taught me how to do, but also how to think and learn. This was great positive to improve myself. The passion and dedication for research that I received from him will inspire me to become a better researcher.

It is my honor to have Dr. Franck Carbonero and Dr. Yi Liang in my committee. I want to express my deep appreciation for their suggestions and help on my research and study.

I would thank the great research group I am in for their help in my research: Dr. Ronghui Wang, for her advice and help on all the research issues; Lisa Kelso, for her help on the training of microbial tests and the revision of papers; Zach Callaway, for his help on my tests; Lizhou Xu and Qinqin Hu, who are visiting scholars from Zhejiang University, China, for their help and advice on biological tests. Lijun Wang, who is a visiting scholars from Nanchang University, China, for her help on microbial tests. I also want to thank the rest of the members in our group for their help in my research and daily life.

I would also want to thank the Department of Biological and Agricultural Engineering and Center of Excellence for Poultry Science for the support that they gave me in my graduate study and research. Especially, I want to express my gratitude to Leland Schrader and James Andress, who work in Department of Biological and Agricultural Engineering as technical assistants, for their help in fabricating the instrument and circuit.

Finally, I want to thank my parents for all they have done for me. I would never reach to this without their love and endless support. Also I want to thank all my friends for their encouragement and help.

Table of Contents

List of Tables

List of Figures

Abbreviations

American Type Culture Collection	ATCC
Antibody	Ab
Avian influenza virus	AIV
Biosafety level	BSL
Brain heart infusion	BHI
Centers for Disease Control and Prevention	CDC
Colony-forming unit	CFU
Data acquisition	DAQ
Deoxyribonucleic acid	DNA
Enzyme-linked immunosorbent assay	ELISA
Hem agglutination units	HAU
Hemolytic Uremic Syndrome	HUS
International Union of Pure and Applied Chemistry	IUPAC
Laboratory Virtual Instrument Engineering Workbench	LabVIEW
Light-emitting diode	LED
Limit of detection	LOD
Magnetic bead	MB

Magnetic nanobead	MNB
Phosphate buffered saline	PBS
Polymerase chain reaction	PCR
Proton beam micromachining	PBM
Quantum dot	QD
Quartz crystal microbalance	QCM
Ready-to-eat	RTE
Separation efficiency	*SE*
Surface acoustic wave	SAW
Surface plasmon resonance	SPR
Virtual instrument	VI

Chapter 1 Introduction

Foodborne diseases are an important public health problem. The spread of animal and plant diseases along with foodborne pathogens can have detrimental effects on crops in agriculture, both animal and human health, and the overall economy of the world. Among foodborne pathogens, bacteria is the second major cause (39%) of foodborne illnesses, the first major cause (64%) of hospitalizations, and the leading cause (64%) of deaths (Xu *et al.*, 2015). And in 2016, 11 cases of multistate foodborne outbreaks related to *E. coli* O157:H7, *Salmonella*, and *Listeria monocytogenes* have been reported by now, they caused 176 people getting sick, 72 of them were hospitalized, and two were dead (CDC, 2016). It can be seen all these cases have caused great damages on the wellbeing of people as well as the revenue and reputation of food industry. Therefore, it is critical to monitor and detect pathogenic bacteria to create healthy sustainable agricultural and food systems.

The conventional culture and colony counting methods are still used as standard techniques to detect foodborne pathogens. Although they are reliable and accurate, the major drawbacks are their labor-intensiveness and time- consuming (Lazcka *et al*., 2007; Velusamy *et al*., 2010). In past years, some rapid detection methods have been reported, such as immunology-based methods including enzyme-linked immunosorbent assay (ELISA) and polymerase chain reaction (PCR) based methods (Malorny *et al*., 2003; Omiccioli *et al*., 2009; Velusamy *et al*., 2010; Mandal *et al*., 2011; Ballarini *et al*., 2013). In recent years, there has been much more research activities in the area of biosensor development for detecting foodborne pathogens (Velusamy *et al*., 2010). The potential application of biosensor technology to food testing offers several attractive features. Many of the systems are portable and hence can be used for field testing or on the spot analysis and are capable for testing multiple samples simultaneously (Mandal *et al*., 2011).

Biosensors can be classified by their bioreceptor (antibody, enzyme, cell, DNA, biomimetic, phage) or their transducer type (optical, mass-based, electrochemical) (Velusamy *et al*., 2010). Among biosensors, fluorescent biosensors have attracted much more attention as they offer many outstanding advantages such as low background noise, high sensitivity and facile sample preparation (Song *et al*., 2014). In recent years, fluorescent semiconductor quantum dots (QDs) have shown significant advantages over traditional organic fluorophores as fluorescent probes, such as resistance to photodegradation, improved brightness, size dependence, narrow-emission spectra, better stability, and high quantum yield (Ozkan, 2004; Yang and Li, 2006; Frasco and Chaniotakis, 2009; Algar *et al.*, 2010; Chidawanyika *et al*., 2010; Liang *et al*., 2015). Many researches using QDs-based biosensor have been reported; however, many of them are still in lab research and not practical for use in the field.

Immunomagnetic separation has been widely used in modern biotechnology and biomedical research fields. This method based on antibodies with high affinity and a bio-specific purification and concentration procedure has always been the most commonly used approach in the area of foodborne pathogen isolation and concentration from complex food matrices (Xu *et al*., 2015). Due to immunomagnetic separation is usually gentle, nondestructive to biological analytes and can be easily used for raw biological samples with several simple steps, this can reduce total analysis time, improve sensitivity and reliability of detection (Bennett *et al*., 1996; Tamanaha *et al*., 2008; He *et al*., 2014).

In this study, a novel automatic and portable biosensing instrument was developed based on our previous research on QD-labeled detection method in lab, and including a target sample extraction function based on immunomagnetic separation method.

Chapter 2 Objectives

The goal of this study was to develop an automatic and portable biosensing instrument that could separate and detect target foodborne pathogen in the field using nanobead-based magnetic separation and quantum dot-labeled fluorescent measurement. And in this research, *E .coli* O157:H7 used as target bacteria.

The specific objectives of this research were:

1. To design and fabricate the integrated biosensing system containing solution delivery, magnetic separation, and fluorescence detection with virtual instrument.
2. To evaluate the biosensing system for its magnetic separation efficiency using surface plating method.
3. To evaluate the biosensing system for its specificity with tests on target and non-target bacteria.
4. To evaluate the biosensing system for its sensitivity with tests on different concentrations of target bacteria.

Chapter 3 Literature Review

3.1 *Escherichia coli* O157:H7

E. coli O157:H7 is an enterohemorrhagic serotype of the bacterium *E. coli*, and is one of the Shiga toxin-producing types of *E. coli*. *E. coli* O157:H7 was first recognized as a human pathogen in two outbreaks of hemorrhagic colitis in 1982 (Mead *et al*., 1998; Besser *et al*., 1999; Fernandez, 2008). Consumption of contaminated foods or unclean water is the most frequent way to transmit *E. coli* O157:H7. Commonly, *E. coli* O157:H7 is associated with ground beef, but other foods also have high risk of carrying the pathogen, such as unpasteurized milk and milk products, unclean leafy green that came in contact with animal feces, and contaminated water (Mead *et al*., 1998; Besser *et al*., 1999). *E. coli* O157:H7 infection can cause vomiting, severe acute hemorrhagic diarrhea and Hemolytic Uremic Syndrome (HUS) (Mead *et al*., 1998; Besser *et al*., 1999; Fernandez, 2008).

Great impact on the public health and the economy can be caused by *E. coli* O157:H7 infections. In the United States, there are over 63,000 estimated cases of *E. coli* O157:H7 infection each year. Among those, about 2,100 of cases led to hospitalization and more than 20 deaths. Those cases also cost over 600 million dollars per year (Scallan *et al.*, 2011; Scharff, 2012). The inspection and monitoring to ensure the safety of food products and reduce the occurrence of foodborne illness caused by *E. coli* O157:H7 has increased due to outbreaks related to this pathogen in recent years caused by the increased consumption of minimally processed products, such as fruits, vegetables, and ready-to-eat (RTE) products (CDC, 2016).

3.2 Magnetic Separation of Bacteria in Food Samples

Magnetic separation is a process in which magnetically susceptible material is extracted from a mixture using a magnetic force. Magnetic beads (MBs) have been widely used in

biotechnology and biomedical research fields. The magnetic beads have the capability to be coated in a variety of chemicals, proteins, or functional groups which can be used in a vast range of applications including separation and purification, molecular detection, cancer research and treatment, drug delivery, and enzymatic reactions. The magnetic beads are usually labeled with antibodies, aptamers, or binding agents to separate target from an environment or clinical sample, such as eukaryotic cells, bacteria, protein, viruses, or food matrices (Øren *et al*., 2005; Jin *et al*., 2009; Lee *et al*., 2009). The separation step in most cases involves the simple act of setting a cuvette containing the fluid and bead suspension next to a permanent magnet for a set amount of time. A layer will be formed with beads when a magnetic field is applied, which allows waste to be separated from the beads and the captured target (Hsing *et al*., 2007). The use of magnetic separation is simple, rapid, inexpensive, and can obtain high capture efficiency and specificity when used with the appropriate binding agent.

Antibody is more often used as agent for magnetic separation. Comparing with other agents, the advantage to use antibody is that it is specific, but usually it is expensive and easy to lose activity. In recent years, aptamer has attracted much more attentions, since it is low cost, desirable for storage (Wang *et al*., 2016).

In recent years, some researches using magnetic beads to isolate target from a sample have been reported, Table 3.1 shows some researches on magnetic separation of bacteria using magnetic beads and antibody in the last five years.

Also, considering the advantages and convenience of magnetic separation, some researchers try to develop and fabricate a device or instrument that can be used in the field based on the theory of magnetic separation. In Figures 3.1 and 3.2, they show two different types of magnetic

separation devices, one is designed using the traditional way, the other is designed with microfluidic technology. Chandler *et al*. (2001) developed an automated immunomagnetic separation system for isolating *E.coli* O157:H7 directly from poultry carcass rinses. The system is shown in Figure 3.1. In the system, a bi-directional syringe pump aspirated beads, sample and/ or reagents into the holding coil through the selection valve for incubation. After incubation, the mixture would be moved to a nickel foam column for magnetic separation, and the captured sample could be collected from the outlet.

Table 3.1 Some researches on magnetic separation of bacteria using magnetic beads and antibody in the last five years.

Target	MBs size (nm)	Capture Conjugate	Capture efficiency (%)	Reference
Salmonella Typhimurium	120	MBs + antibody	Not available	Joo *et al*., 2012
Listeria monocytogenes	30	MBs + antibody	75	Kanayeva *et al*., 2012
E.coli O157:H7	150	MBs + antibody	Not available	Luo *et al*., 2012
E.coli O157:H7	1080	MBs + antibody	Not available	Chan *et al*., 2013
Salmonella	100	MBs + antibody	90	Kuang *et al*., 2013
Staphylococcus aureus	100	MBs + antibody	96 in PBS 78 in milk	Sung et al., 2013
Salmonella Typhimurium *E.coli O157:H7* *Listeria monocytogenes*	180	MBs + antibody	>70	Yang *et al*., 2013
Listeria monocytogenes	180	MBs + antibody	94.12	Shan *et al*., 2014
Campylobacter jejuni	150	MBs + antibody	Not available	Wang *et al*., 2014
Salmonella Typhimurium	300	MBs + antibody	Not available	Brandão *et al*., 2015
Salmonella Typhimurium	20	MBs + antibody	Not available	Kim *et al*., 2015

Table 3.1(Cont.) Some researches on magnetic separation of bacteria using magnetic beads and antibody in the last five years.

Target	MBs size (nm)	Capture Conjugate	Capture efficiency (%)	Reference
E.coli O157:H7	150	MBs + antibody	Not available	Kwon *et al*., 2015
E.coli O157:H7	30 180	MBs + antibody	>90	Li *et al*., 2015
E.coli O157:H7	300	MBs + antibody	>95	Martelet *et al*., 2015
E.coli O157:H7 *Salmonella* Typhimurium *Listeria monocytogenes* *Staphylococcus aureus*	25	MBs + antibody	>87.5	Xu *et al*., 2015
Mycobacterium avium subsp.	100	MBs + antibody	96.44±0.77	Kim *et al*., 2016
Campylobacter spp.	2800	MBs + antibody	Not available	Romero *et al*., 2016
Cronobacter sakazakii	30	MBs + antibody	88.23	Shukla *et al*., 2016
Staphylococcus aureus	3000	MBs + antibody	Not available	Yu *et al*., 2016
Enterobacter cloacae	200	MBs + antibody	91	Zhang *et al*., 2016

In Figure 3.2, Qiu *et al*. (2009) developed a magnetic separation –based microfluidic device for isolating *Salmonella*. In this device, magnetic beads was introduced into microchannels from A or B inlet using a syringe, and then the sample was pumped through the chip from E inlet. Simultaneously, other inlets (except F) were continuously filled with “buffer A” to keep the sample flowing circularly in the U-type microchannel. Finally, target would be isolated from the sample when the mixture passes through the magnet field.

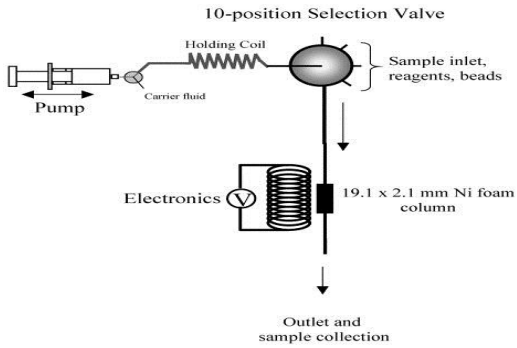

Figure 3.1 Schematic diagram of the sequential injection renewable separation column (SI-RSC) system (From Chandler *et al*., 2001. Used with permission from Elsevier).

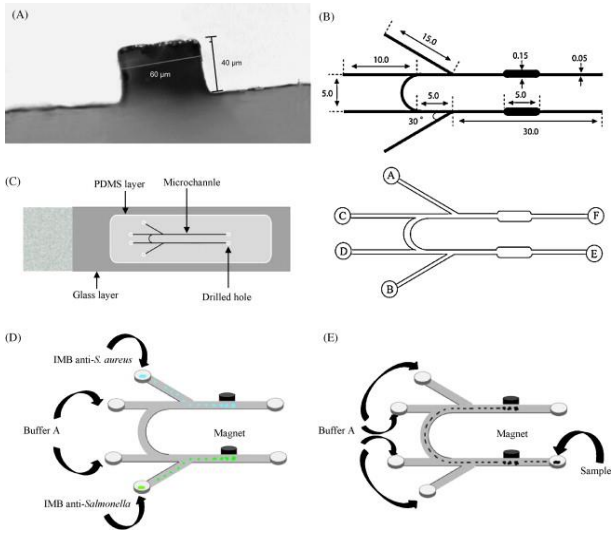

Figure 3.2 The schematic diagram of the microfluidic device. (A) The depth and width of the microchip. (B) Layout of the U-type microchip used for separation and detection of bacteria. Dimensions (in mm) correspond to the photomask features. Reservoirs A–B, C–D and E represent the inlets of IMB, buffer solutions and bacterial sample, respectively, and F is the outlet. (C) The appearance of the PDMS/glass microfluidic chip. (D) IMB is pumped to the channel for capture with a magnet. (E) The sample (bacteria and FITC-labeled antibodies) is introduced from reservoir E. Beads show as blue and green streaks, sample as dark staff (From Qiu *et al*., 2009.Used with permission from Elsevier).

3.3 Current Methods of Foodborne Pathogen Detection

Conventional bacterial detection methods are based on specific microbiological media to isolate and enumerate target bacterial cells in foods. These methods are also known as "gold standard methods" because of they are the only one that will recover all the viable microbes from

a sample. Also, they can offer many advantages, such as high sensitivity, low cost, and they can provide both qualitative and quantitative information on the number and the nature of microorganisms present in the food sample. However, they typically require many steps that consume too much time such as enrichment and incubation before they are actually measured, which could make testing time last several days. (de Boer and Beumer, 1999; Mandal *et al*., 2011; Valderrama *et al*., 2016).

In recent years, many methods have been developed for rapid detection of foodborne pathogens in food samples, such as simple polymerase chain reaction (PCR), multiplex PCR, real –time PCR, enzyme-linked immunosorbent assay (ELISA) (Mandal *et al*., 2011; Zhao *et al*., 2014; Law *et al*., 2015; Valderrama *et al*., 2016). Although these methods are rapider comparing with conventional bacterial testing methods, they are still time consuming including labor required for the analysis since an additional enrichment step in a medium to grow target pathogens or pretreatment to perform the extraction of suitable target DNA from target bacteria is required. (Malorny *et al*., 2003; Omiccioli *et al*., 2009; Velusamy *et al*., 2010; Mandal *et al*., 2011; Ballarini *et al*., 2013).

3.4 Biosensors for Bacteria Detection

The first biosensor was reported in 1962 by scientist Leland C. Clark with the development of enzyme electrodes for the detection of glucose (Mohanty and Kougianos, 2006). Since then, many researchers form different field have come together to develop more sophisticated, reliable, and mature biosensing devices (Mohanty and Kougianos, 2006). In recent years, the development of the modern information and nano technology make it is possible to develop

rapid, sensitive and real-time biosensors for foodborne pathogens detection (Seo *et al*., 1998; Arora *et al*., 2011).

A biosensor is a device or instrument that utilizes biological sensing material corresponded to a chemical or physical transducer which can convert the biological, chemical, or biochemical signal into a quantifiable and easily processed electrical signal (Li, 2006; Yogeswaran and Chen, 2008; Sharma and Mutharasan, 2013). A more accurate definition of biosensor made by The International Union of Pure and Applied Chemistry is "a device that uses specific biochemical reactions mediated by isolated enzymes, immunosystems, tissues, organelles or whole cells to detect chemical compounds usually by electrical, thermal, or optical signals" (IUPAC, 1997).

In Figure 3.3, it shows the typical structure and components of a biosensor. The biological sensing material of a biosensor might be enzymes, antibodies, cells, organelles, phage, tissue or biomimetic material, while the transducer types could be electrochemical, optical, acoustical, piezoelectric, magnetic, mass-based or mechanical (Turner *et al*., 1987; Velusamy *et al*., 2010) .

Biosensors can detect a wide range of targets from small protein molecules to large pathogens and have been widely applied in agricultural production, food processing, drug analysis, clinical diagnostics and environmental monitoring. Compared to the conventional methods, a biosensor device could be used for detection of foodborne pathogens without requiring highly trained personnel. Further, considering the advantages of accuracy, near real-time assay, sensitivity, specificity, reproducibility, and robustness, biosensors are more ideal for practical and field applications than conventional methods (Sharma and Mutharasan, 2013).

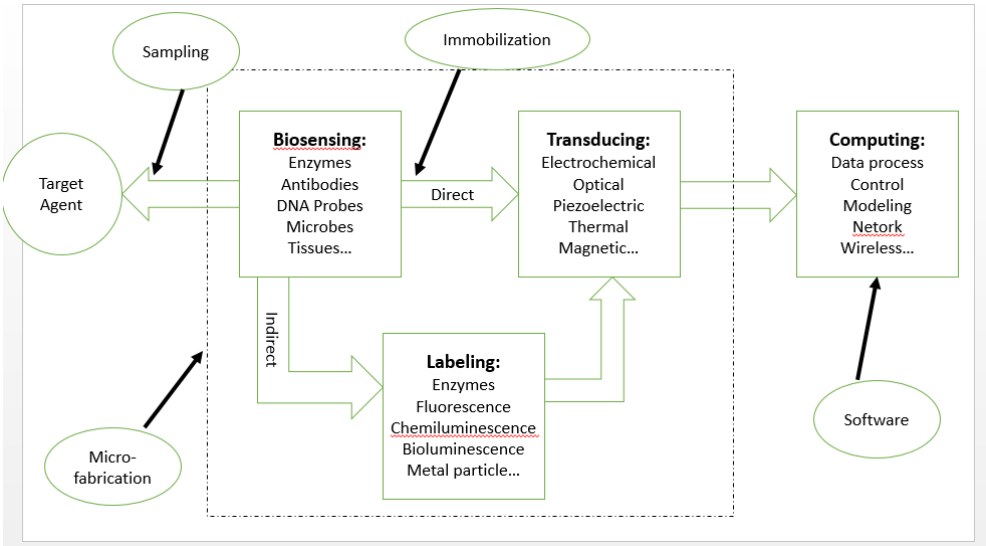

Figure 3.3 Typical structure and components of a biosensor (Li, 2006. Used with permission from ASABE).

3.4.1 Major Types of Biosensors

The biosensors used in the area of foodborne pathogens could be classified into three major types based on their transducer type: optical, piezoelectric and electrochemical.

The principle of an optical biosensor is the use of optical phenomenon to indicate the interaction between the target and the biological probe of the biosensor. A typical optical biosensor includes three parts: a light source, a modified sensing head, and a photodetector. Optical biosensors can consist of a fluorescent sensor, an absorption sensor, an evanescent field fiber optic biosensor, a luminescence or a surface plasmon resonance (SPR) sensor. Generally, there are two detection protocols that can be applied in optical biosensing: direct and indirect detection of the target analyte. The direct format is also named label-free detection. In this format, the optical properties of a waveguide are directly affected by the target analyte and the target analyte is detected in natural forms. In indirect format, optical signal proportional to the target analyte is generated by optical labels (Li, 2006; Fan *et al*., 2008; Arora *et al*., 2011; Sharma and Mutharasan, 2013).

The principle of piezoelectric biosensor involves mass changes on the crystal surface which can lead to the changes in resonant frequency of a piezoelectric crystal. The concentration of a target can be indicated through measuring the changes of frequency. A typical piezoelectric biosensor includes a quartz crystal wafer and two excitation electrodes plated on opposite sides of the crystal. Generally, there are two major types of piezoelectric devices: quartz crystal microbalance (QCM), operating at frequencies below 15 MHz, and surface acoustic wave (SAW), operating at frequencies above 100 MHz (Bunde *et al*., 1998; Li, 2006; Arora *et al*., 2011).

The principle of an electrochemical biosensor involves interactions that occur between the target analyte and the sensor electrode interface which can produce or consume ions or electrons, causing changes in the electrical properties of the solution and resulting in the changes of current, potential or impedance. The concentration of a target analyte can be reflected through the changes of current or potential. Based on the measured parameter, electrochemical biosensor can be further divided into amperometric/ voltammetric (current), potentiometric (potential), and conductivity/ capacitance/ impedimetric (impedance) (Li, 2006; Mohanty and Kougianos, 2006; Arora *et al*., 2011; Sharma and Mutharasan, 2013; Bhardwaj, 2015).

Among all these types of detection, optical biosensors have experienced an exponential growth in application during the last decade and have been widely applied on quantitative proteomic analysis and infectious disease diagnostics due to the considerable advantages of high specification (Rusling *et al*., 2010; Foudeh *et al*., 2012).

3.4.2 Quantum Dot-Based Fluorescent Biosensors

Fluorescence is a widely used tool in optical biosensors since its low background noise, high sensitivity, and selectivity are advantageous (Velasco-Garcia, 2009; Song *et al*., 2014). The principle of fluorescent biosensors involve that fluorescent tags that are labeled with the target molecules or biorecognition molecules in order to indicate the concentration of the target molecules or the interaction strength between target and biorecognition molecules (Fan *et al*., 2008). Therefore a suitable fluorescent tag is the key for a fluorescent biosensor. A suitable tag should be bright, sufficiently stable under relevant conditions, available in a reproducible quality, compatible for signal-amplification strategies, soluble in relevant buffers, cell culture media or body fluids, and have functional groups for site-specific labeling (Resch-Genger *et al*., 2008). Traditional organic dyes, such as phycobiliproteins and encoded fluorescent proteins, were the most widely used fluorescent label at one time. In recent years, with the development of nano technology, the nanocrystal label -- fluorescent semiconductor quantum dots (QDs) have attracted much attention in research.

Quantum dots are tiny particles or nanocrystals of a semiconducting material with diameters in the range of 2-10 nanometers (10-50 atoms), and were first synthesized in 1980 (Ekimov and Onushchenko, 1981). Quantum dots display unique electronic properties, intermediate between those of bulk semiconductors and discrete molecules that are partly the result of the unusually high surface-to-volume ratios for these particles. The most apparent advantage of the quantum dot is that it can produce distinctive colors determined by the size of the particles (Kasfner, 1993; Ashoori, 1996; Collier *et al*., 1998). Compared with traditional organic fluorophores, quantum dots have many advantages, such as resistance to photodegradation, improved brightness, size dependence, narrow-emission spectra, better stability, good applicability to single-molecule

analysis, and high quantum yield (Ozkan, 2004; Yang and Li, 2006; Resch-Genger *et al*., 2008; Frasco and Chaniotakis, 2009; Algar, 2010; Chidawanyika *et al*., 2010; Liang *et al*., 2015;).

In the past decade, many researches on quantum dot-based fluorescent biosensors for detection bacteria have been reported, as shown in Table 3.2.

Besides the applications listed above, researchers are developing and fabricating a device or instrument that could be used in field based on the quantum dots-labeled fluorescent biosensor. Two different types of portable quantum dot-based fluorescent biosensor instruments that may be used in field are shown below.

Zhu *et al.* (2012) have reported a cell-phone based *E. coli* detection platform based on quantum dots as shown in Figure 3.4. In this platform, to perform a quantum dot based sandwich assay for specific detection of *E. coli* O157:H7 in a liquid sample, the anti-*E. coli* antibody functionalized glass capillaries were used as solid substrates. The captured labeled *E. coli* particles were excited through light-emitting-diodes (LEDS), and the cellphone camera unit was used to image the emission from the quantum dots through an additional lens that was inserted between the capillary and the cellphone. The concentration of target bacteria in the sample was determined by quantifying the fluorescent light emission from each capillary tube. The limit of detection of this platform was about 5 to 10 CFU/mL in buffer solution and fat-free milk.

Kim *et al*. (2015) developed a nano-biosensor system to rapidly detect *Salmonella* based on quantum dots. In this biosensor system, a microfluidic chip was used to separate and concentrate the cells from the sample as shown in Figure 3.5, and a portable fluorometer was developed to measure the fluorescence signal as shown in Figure 3.6. The immunomagnetic separation method was used first to capture the target cells from sample, then the captured cells and antibody-

conjugated QDs were injected to the inlet ports 1 and 2 of the microfluidic chip, respectively. Next, the two solutions were mixed in the meandering channel through negative pressure generated by a peristaltic pump, and the cells were labeled with the antibody-conjugated QDs. Finally, the QDs-labelled cells were captured in the detection zone using an external fixed magnet placed under the detection zone, and the unbound QDs were removed by injecting borate buffer into two inlet ports. The microfluidic chip was then inserted into the portable fluorometer for measurement. The limit of detection for this system to detect *Salmonella* was 10^3 CFU/mL.

Table 3.2 Some researches on quantum dot-based biosensors for detection of bacteria in the past ten years.

Target	Limit of Detection	Reference
Bacillus thuringiensis Spores	10^3 CFU/mL	Ikanovic *et al*., 2007
Listeria monocytogenes	2~3 CFU/mL	Wang *et al*., 2007
Salmonella typhimurium *Shigella flexneri* *Escherichia coli* O157:H7	10^3 CFU/mL 10^3 CFU/mL 10^3 CFU/mL	Zhao *et al*., 2008
Escherichia coli	10^4 CFU/mL	Mukhopadhyay *et al*., 2009
E.coli O157:H7 *Staphylococcus aureus*	10^2 CFU/mL	Xue *et al*., 2009
E.coli	28 CFU/mL	Carrillo-Carrión *et al*., 2011
Escherichia coli	10^4 CFU/mL	Duplan *et al*., 2011
E.coli O157:H7	10 CFU/mL	Sanvicens *et al*., 2011
E.coli O157:H7 *Salmonella* Typhimurium *Listeria* monocytogenes	20~ 50 CFU/mL	Wang *et al*., 2011
E.coli O157:H7 *Salmonella*	10 CFU/g	Wang *et al*., 2012
Pseudomonas aeruginosa *Staphylococcus aureus*	200 CFU/mL 150 CFU/mL	Abdelhamid and Wu, 2013
E.coli O157:H7 *Salmonella* Typhimurium	3 CFU/mL 5 CFU/mL	Cho and Irudayaraj, 2013

Table 3.2 (Cont.) Some researches on quantum dot-based biosensors for detection of bacteria in the past ten years.

Target	Limit of Detection	Reference
Vibrio parahaemolyticus *Salmonella* Typhimurium	5×10^3 CFU/mL	Duan *et al.*, 2013
E.coli O157:H7 *Salmonella* Typhimurium *Listeria* monocytogenes	10^3 CFU/mL	Yang *et al.*, 2013
Staphylococcus aureus	3×10^0 CFU/mL in spiked milk powder 3×10^1 CFU/g in meat samples	Chen *et al.*, 2014
Staphylococcus aureus	10^3 CFU/mL	Hu *et al.*, 2014
Salmonella Enteritidis	10^2 CFU/mL	Wang *et al.*, 2014
Campylobacter jejuni	2~3 cells/0.1 mL	Wang *et al.*, 2014
Vibrio parahaemolyticus *Salmonella* Typhimurium *Staphylococcus aureus*	10^2 CFU/mL	Wu *et al.*, 2014
E.coli O157:H7 *Salmonella* Typhimurium *Listeria* monocytogenes *Staphylococcus aureus*	80, 160, 47, 100 CFU/mL	Xu *et al.*, 2015
E.coli	30 CFU/mL	Dogan *et al.*, 2016

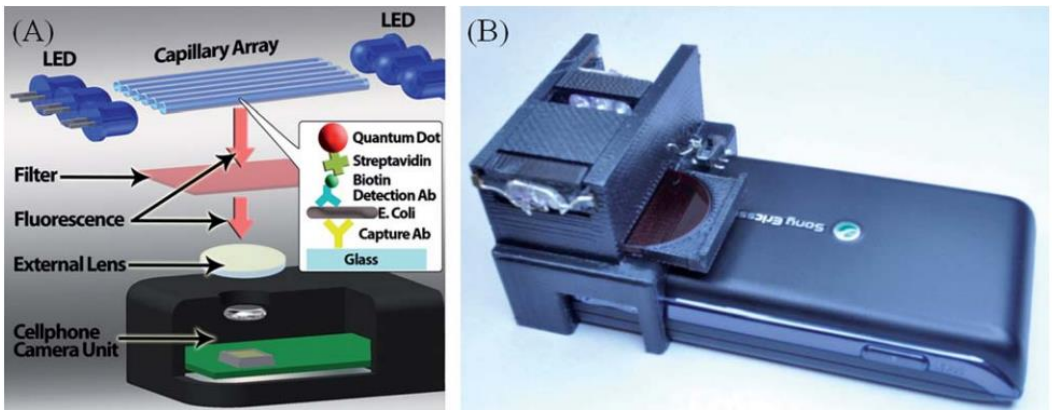

Figure 3.4 (A–B) Schematic diagram and picture of the optical attachment for *E. coli* detection on a cell-phone using the quantum dot based sandwich assay in glass capillary tubes (Zhu *et al.*, 2012. Used with permission from Royal Society of Chemistry).

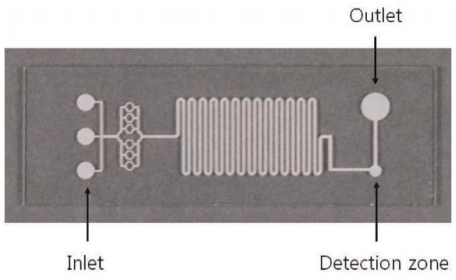

Figure 3.5. Layout of the microfluidic channel (Kim *et al*., 2015. Used with permission from Elsevier).

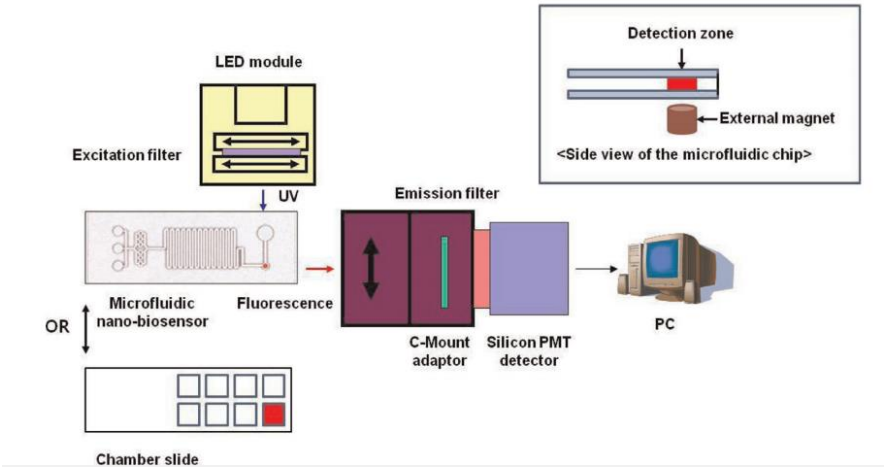

Figure 3.6 Schematic diagram of the portable fluorometer (Kim *et al*., 2015. Used with permission from Elsevier).

3.5 Commercial Biosensor Instruments for the Detection of Foodborne Pathogens

Biosensor technologies have high potential in developing portable and automated equipment combining with intelligent instrumentation, electronics, and multi-variate signal processing methods. In recent years, several commercial biosensor instruments have been developed.

As shown in Figure 3.7, RABIT (rapid automated bacterial impedance technique), which is made by Don Whitley Scientific Ltd (Shipley, UK), is a direct and indirect impedance measurement system for the rapid detection of bacteria, yeasts and molds. The system is designed to allow tests to be carried out over a range of incubation temperatures to provide

maximum flexibility for microbiological testing. This instrument uses the direct technique to measure the changes of metabolizing micro-organisms as they increase electrical conductance of the culture media in the system, and the indirect technique is used to monitor the amount of carbon dioxide produced by growing organisms. In addition, it has a Windows™-based software for easy sample entry and analysis of results (Don Whitley Scientific Ltd).

Figure 3.8 shows an instrument named PR610-2™. It is a flexible, robotic, fluorometric assay system designed and built by Research International, Inc (Monroe, Washington). It is used for the high-sensitivity monitoring of food-borne pathogens and their toxins. Optics, fluidics, robotics, and software are integrated into this system. It will automatically perform a user-defined, multi-step, fluoro-immunoassay protocol on 1 to 4 different samples by means of each of the system's four disposable optical waveguide sensors. And *E .coli* O157:H7 can be detected from 100 to 1000 CFU/mL (Research International, Inc).

The Aegis 1000, as shown in Figure 3.9, which is made by Biodetection Instruments, LLC (Fayetteville, AR), is an automatic cartridge-based assay device. It uses highly efficient capillary bioseparators/bioreactors that specifically capture and separate target biological and/or chemical agents (including bacteria, viruses, proteins, toxins, pesticides, antibiotics, etc.) from food, water, environmental, or clinical samples and quickly generates quantitative optical signals. The cartridge is designed to be self-contained, easy to use, and cost-effective for mass production and disposable use. The system can simultaneously finish quantitative analyses of multiple samples/agents in less than one hour, and has a touch-screen for users to monitor the process (Biodetection Instruments, LLC).

Figure 3.7 Picture of a RABIT instrument (Don Whitley Scientific Ltd. Used with permission).

Figure 3.8 Picture of a PR610-2™ instrument (Research International, Inc. Used with permission).

Figure 3.9 Picture of an Aegis 1000 instrument (Biodetection Instruments, LLC. Used with permission).

3.6 LabVIEW Software Applications

Since LabVIEW is a powerful toolset for process control, data fitting and signal processing, and has fast, easy and friendly user interface construction (Elliott *et al*., 2007), it has widely used in research and industry in recent years. For example, Bettiol *et al*. (2001) developed a

LabVIEW-based scanning and control system for a proton beam micromachining (PBM) application; Salehi and Brandt (2006) developed a LabVIEW-based temperature control system to control the temperature of a melt pool; Nikitin and Rao (2009) developed a UHF radio-frequency-identification tag test and measure*m*ent system based on LabVIEW; Zhang *et al*. (2013) developed a LabVIEW-based impedance analyzer using the audio card from a laptop for avian influenza virus (AIV) detection.

Chapter 4 Materials and Methods

4.1 Materials

4.1.1Biological and Chemical Reagents

The Millipore water purification system (Mill-Q, Bedford, MA) provided all the water used in this study. Phosphate buffered saline (PBS, 10X) was purchased from Sigma-Aldrich (St. Louis, MO) and diluted with Milli-Q (Mill-Q, Bedford, MA) water to 10 mM (pH 7.4) for use in all tests.

Biotin-labeled rabbit polyclonal anti-*E. coli* O157:H7 antibody was purchased from Meridian Life Science (Memphis, TN) and diluted to 0.4-0.5 mg/ml with PBS for use in all tests. Streptavidin-coated 150 nm magnetic nanobeads (MNBs) were obtained from Ocean NanoTech (San Diego, CA). The MNBs were iron oxide crystals with a magnetite structure (Fe_3O_4). The streptavidin coating was attached to polymer, adding about 4 nm to the total nanobeads diameter. The concentration of the MNBs was 2.02×10^{13} particles/mg. The CdSe/ZnS Core/Shell streptavidin-coated quantum dots (QDs) with emission wavelength of 614 nm was obtained from Ocean NanoTech (San Diego, CA). The concentration of the QDs was 1μM. *Escherichia coli* O157:H7 was purchased from American Type Culture Collection (ATCC 43888) and stored in brain heart infusion broth (BHI, Remel Inc., Lenexa, KS) at -80 °C. 1.5 mL low binding tubes were purchased from Sarstedt (Nümbrecht, Germany). The borosilicate glass culture tubes with size 6 × 50 mm were purchased from VWR (West Chester, PA).

4.1.2 Mechanical and Electronic Parts

As shown in Figure 4.1 (a), the micro pump SP 100 series with the dimensions 60 × 47 × 74 mm (W × H × D), powered by a 12 V DC at 75 to 300 mA, was purchased from APT Instruments (Rochester, IL). The accuracy and repeatability of the pump are both ±10% full

scale. The flow rate varies depending upon the tubing dimension, fluid viscosity, and back pressure. The tubing purchased from Emco Industrial Plastic, Inc. (Cedar Grove, NJ) was used to connect the reaction tubes with pumps.

The stepper motor NEMA-17 was purchased from Adafruit (New York City, NY). It is a 4-wire bipolar stepper motor, as shown in Figure 4.1 (b), which can be operated in half step mode with 0.9 degree each step or full step mode with 1.8 degree each step. The sequence for full step and half step are shown in Table 4.1 to Table 4.4, respectively. In these tables, the 1 represents high electrical level and the 0 represents low electrical level.

(a) (b)

Figure 4.1 (a) The micro pump SP 100 series and (b) stepper motor NEMA-17.

Table 4.1 Full step sequence (clockwise) used for controlling stepper motor.

	IN1	**IN2**	**IN3**	**IN4**
State 1	1	0	0	0
State 2	0	0	1	0
State 3	0	1	0	0
State 4	0	0	0	1
State 5	1	0	0	0

Table 4.2 Full step sequence (counterclockwise) used for controlling stepper motor.

	IN1	**IN2**	**IN3**	**IN4**
State 1	0	0	0	1
State 2	0	1	0	0
State 3	0	0	1	0
State 4	1	0	0	0
State 5	0	0	0	1

Table 4.3 Half step sequence (clockwise) used for controlling stepper motor.

	IN1	IN2	IN3	IN4
State 1	1	0	0	0
State 2	1	0	1	0
State 3	0	0	1	0
State 4	0	1	1	0
State 5	0	1	0	0
State 6	0	1	0	1
State 7	0	0	0	1
State 8	1	0	0	1
State 9	1	0	0	0

Table 4.4 Half step sequence (counterclockwise) used for controlling stepper motor.

	IN1	IN2	IN3	IN4
State 1	0	0	0	1
State 2	0	1	0	1
State 3	0	1	0	0
State 4	0	1	1	0
State 5	0	0	1	0
State 6	1	0	1	0
State 7	1	0	0	0
State 8	1	0	0	1
State 9	0	0	0	1

SN74ls138 and SN74ls04 chips were purchased from Texas Instrument (Dallas, TX), as shown in Figure 4.2 (a) and (b), respectively. SN74ls138 is a 3-line to 8-line decoder. It decodes one of eight lines, which is dependent on the conditions of the three binary select inputs and the three enable inputs. Table 4.5 shows the function table of SN74ls138. SN74ls04 is an inverter chip with six independent inverters.

L298N chip was purchased from STMicroelectronics, Inc (Geneva, Switzerland), as shown in Figure 4.2 (c). It is a dual full-bridge driver with high voltage and high current. And it is designed to accept standard transistor–transistor logic (TTL) electrical level and drive inductive loads such as relays, solenoids, DC and stepper motors. It has two enable inputs which are used

to enable or disable the input signals independently. The emitters of the lower transistors of each bridge are connected together and the corresponding external terminal can be used for the connection of an external sensing resistor. An additional lower voltage supply input is provided so that the logic works at a safe range (STMicroelectronics, 2000).

Relays, resistors and capacitors were purchased from Digi-Key Corporation (Thief River Falls, MN).

Table 4.5 The function table of SN74ls138 (Texas Instruments, 1998) used to expand I/O ports.

INPUTS					**OUTPUTS**							
ENABLE		**SELECT**										
G1	$\bar{G}$ 2	C	B	A	Y0	Y1	Y2	Y3	Y4	Y5	Y6	Y7
X	H	X	X	X	H	H	H	H	H	H	H	H
L	X	X	X	X	H	H	H	H	H	H	H	H
H	L	L	L	L	L	H	H	H	H	H	H	H
H	L	L	L	H	H	L	H	H	H	H	H	H
H	L	L	H	L	H	H	L	H	H	H	H	H
H	L	L	H	H	H	H	H	L	H	H	H	H
H	L	H	L	L	H	H	H	H	L	H	H	H
H	L	H	L	H	H	H	H	H	H	L	H	H
H	L	H	H	L	H	H	H	H	H	H	L	H
H	L	H	H	H	H	H	H	H	H	H	H	L

Note: $\bar{G}$ 2 = $\bar{G}$ 2A +$\bar{G}$ 2 B

H =high level, L=low level, X=irrelevant

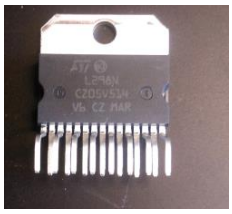

(a) (b) (c)

Figure 4.2 (a) SN74ls138, (b) SN74ls04 and (c) L298N.

4.1.3 A Laptop and A DAQ Card

A laptop of Dell (Round Rock, TX) was used with LabVIEW 2012 software (National Instruments, Austin, TX) and fluorescent detection software (Dunedin, FL) installed. The selected data acquisition (DAQ) card, USB-1208fs, was purchased from Measurement Computing Corporation (Norton, MA), as shown in Figure 4.3.

Figure 4.3 Picture of a USB-1208fs DAQ card.

4.2 Methods

4.2.1 Surface Plating Method

Stock culture of *E. coli* O157:H7 from -80 °C was grown in brain heart infusion broth (BHI) at 37 °C for 18 h. For enumeration, the culture was serially diluted in PBS and then 0.1 mL of proper dilution was plated on tryptic soy agar (TSA, BD Biosciences, Franklin Lakes, NJ). The colonies was counted to determine the number of viable cells in terms of colony forming units per milliliter (CFU/mL) after the plate was incubated at 37 °C for 22-24 h.

In experiments of magnetic separation, the uncaptured cells, captured cells and the original culture were determined by this method. The separation efficiency (*SE*) was calculated with the following equation:

$$SE = \frac{N_c}{N_o} \times 100 \quad (1)$$

where N_c is the number of captured cells, and N_o is the number of original cells.

Due to biosafety concerns, all bacteria tests were handled in a BSL 2 laboratory with trained personnel and the culture was diluted and placed in a boiling water bath for 10-15 min to kill bacterial cells for use in detection tests with the biosensing instrument.

4.2.2 Food Samples Preparation and Inoculation

25 g sample of raw ground beef (purchased from a local grocery store) mixed with 225 mL of PBS in a filter bag. Then, the filter bag was put into a stomacher (Stomacher 400, Seward, U.K.) for 1 min at 200 rpm. After this, the wash solution from the filter bag was collected and then centrifuged for 5 min at 1500 rpm in order to remove the large size components in food matrix. Finally, the inoculation concentrations of *E. coli* in ground beef wash solution were 10^3 -10^7 CFU/mL.

4.2.3 Principle of Nanobead-Based Magnetic Separation and Quantum Dot-Labeled Fluorescent Measurement

As shown in Figure 4.4, magnetic nanobead-antibody (MNB-Ab) conjugates were used to capture *E. coli* O157:H7 and form MNB-Ab-cell complexes first. Then quantum dot-antibody (QD-Ab) conjugates were added as fluorescent labels to form MNB-Ab-cell-Ab-QD sandwich structures. Finally, fluorescent detector was used to measure fluorescent intensity. The concentration of bacteria was determined based on the fluorescent intensity.

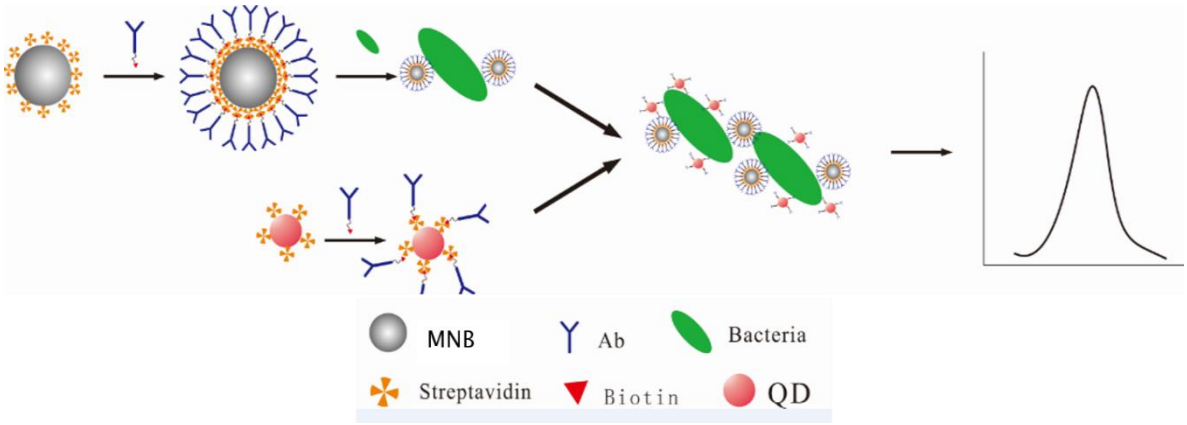

Figure 4.4 Detection of foodborne pathogens using nanobead-based magnetic separation and quantum dot-labeled fluorescent measurement.

4.2.4 Preparation of Magnetic Nanobead-Antibody Conjugates

MNB-Ab conjugates were prepared by binding streptavidin-coated MNBs with biotin-labeled anti-*E. coli* antibodies via biotin-streptavidin coupling strategy, as shown in Figure 4.5. Briefly, 20 µL of MNBs were washed with 200 µL of PBS in a low binding tube. After 3 min magnetic separation, the nanobeads were resuspended in 170 µL of PBS. The resuspended MNBs were mixed with 10 µL of biotin-labeled anti-*E. coli* antibodies and incubated for 30 min at room temperature using a rotating mixer (Grant Instruments, UK) at 10 rpm. After this, another 3 min magnetic separation was applied to remove all unbound antibodies. Once this was completed, MNBs-Ab conjugates were resuspended in 30 µL of PBS and stored at 4 °C for further use.

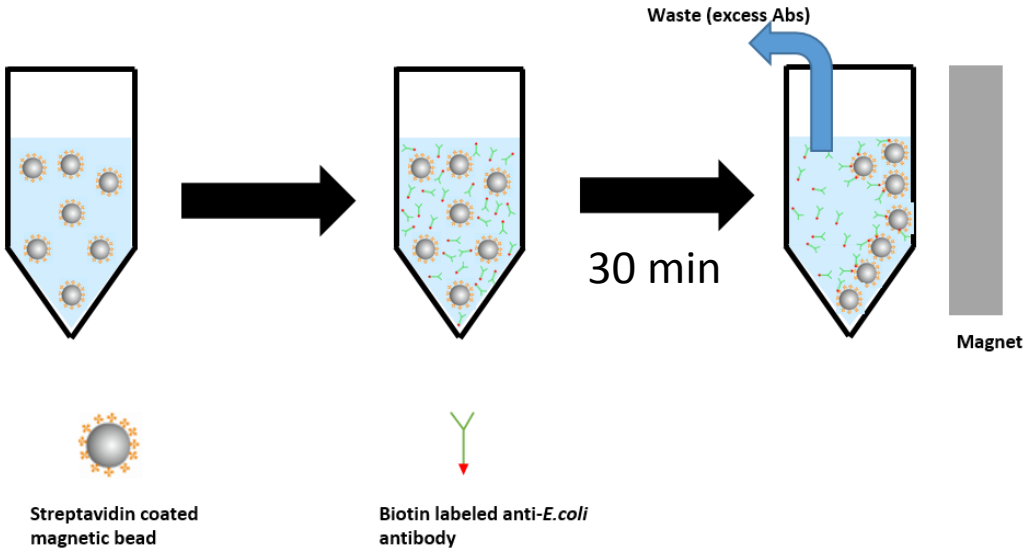

Figure 4.5 Preparation of the nanobeads-antibody conjugates.

4.2.5 Preparation of Quantum Dot-Antibody Conjugates

As shown in Figure 4.6, QD-Ab conjugates were prepared with following steps. First, 5 µL of biotin-labeled anti-*E. coli* antibodies and 10 µL of streptavidin-labeled QDs with emission wavelength of 614 nm were mixed in a low binding tube with 185 µL of PBS. And then incubated for 40 min at room temperature using a rotating mixer at 10 rpm. After this, QDs-Ab conjugates were stored at 4 °C for further use.

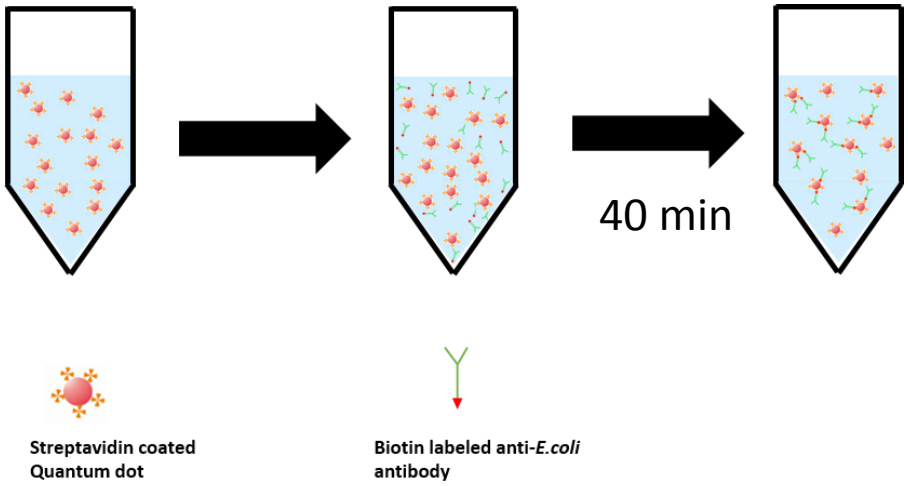

Figure 4.6 Preparation of the quantum dots-antibody conjugates.

4.2.6 Preparation of the Reaction Tube

As shown in Figure 4.7, the reaction tubes were low binding tubes on which four holes were drilled in order to meet the needs in experiments. Totally three holes on the top, the biggest one was used to connect the air pressure pump, and others were used to connect the PBS and QDs pumps. The size of these three holes should a little smaller than outer diameter of the tubing. The hole at the bottom was used as an outlet for the waste and test solution to be pushed from the top to the bottom. And the size of this hole was optimized to make sure the solution can be flushed easily without air bubble, which can cause error on the measurement, and the negative air pressure can hold the solution in reaction tubes.

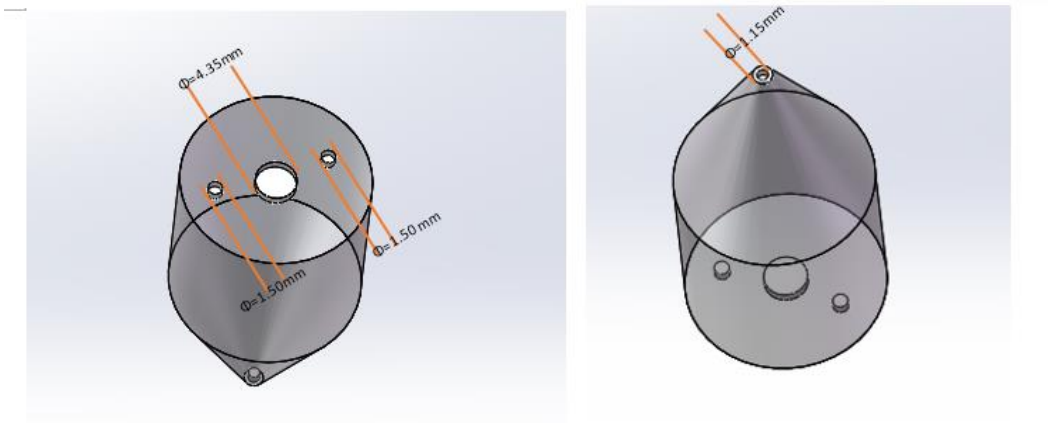

(a) (b)

Figure 4.7 A diagram of the reaction tube used to hold sample solution (a) Top view and (b) bottom view.

4.2.7 Fluorescent Measurement

A portable fluorescent detector purchased from Ocean Optic (Dunedin, FL) was used for fluorescent measurement as shown in Figure 4.8. It included a USB-2000 fiber-optic detector with a range of 360 to 900 nm, a UV LED pulsed LS-450 light source with an excitation

wavelength of 380 nm, an R400-7 UV-visible optical reflection/backscattering probe and fluorescence measurement software. The probe was inserted into the detection box through a hole, as shown in Figure 4.9. The sample solution was placed into borosilicate glass culture tubes for measurement. The fluorescence signals were collected in dark environment, and finally the data was processed by fluorescence measurement software.

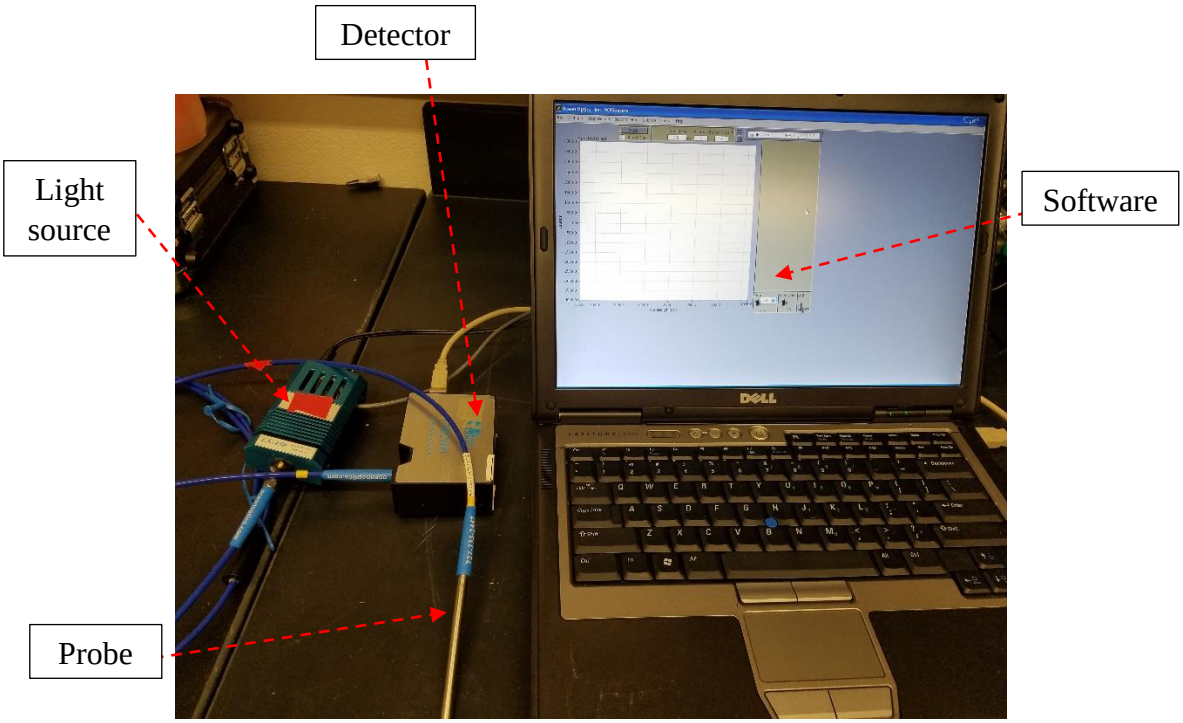

Figure 4.8 Picture of the portable fluorescent measurement system used for fluorescent detection.

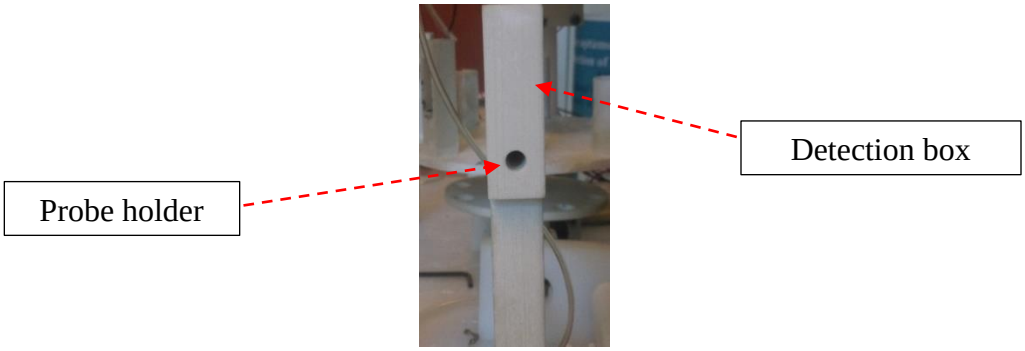

Figure 4.9 Picture of the detection box used to hold probe in fluorescent measurement system.

4.2.8 Statistical Analysis

The means ± standard deviations of fluorescent intensities were calculated using Microsoft Excel software (Microsoft Corporation, Redmond, WA). Using a confidence of 95%, *t*-tests and linear regression were performed for data processing. Means were considered significantly different at $P < 0.05$.

Chapter 5 Results and Discussion

5.1 The Biosensing System

As shown in Figure 5.1, the biosensing system we developed consisted of three parts: mechanical device, electronic circuit and control software. LabVIEW was used to develop a system control software as a virtual instrument (VI) working with the DAQ card and circuit to control the pumps and platforms. Also this software could control fluorescent measurement software. The laptop was where all of the measured data was processed and saved. The DAQ and circuit were used as a bridge for the communication between the laptop and the device. The mechanical part could be divided into two parts, one was a sample treatment module used for magnetic separation and incubation, the other was a detection module used for fluorescence measurement.

There were two prime data flows in this system: the input line and the output line. In the input line, the measured data were collected by the fluorescent measurement software and saved in an excel file. The output line could transport the instructions from the laptop through the DAQ to the specific electronic circuit to control the platforms and pumps. The air pressure pumps and reaction tubes were connected by tubing with a 4.0 mm inner diameter. The PBS and QDs pumps were connected to reaction tubes by tubing with a 0.8 mm inner diameter. The stepper motors could be controlled with 1.8 or 0.9 degree each step in different conditions.

5.2 Mechanical Device

The mechanical device consisted of pumps, stepper motors, platforms, a detection box and a magnet as shown in Figure 5.2. It could be divided into two parts, the top part for magnetic separation and incubation and the bottom part mainly for fluorescent detection.

The platforms and detection box were printed by a 3D printer. The reaction tubes were held in the top platform, and the bottom platform was responsible for waste collection and fluorescent detection. Stepper motors were used to move platforms, detection box, and magnet to expected position. For air pressure pumps, they could generate negative air pressure to hold and mix the solution in reaction tube or generate positive air pressure to push solution from top to bottom. The PBS pumps and QDs pumps were used for adding PBS solution and QD-Ab conjugates solution into reaction tubes, respectively. The magnetic flux density of the magnet was 1 Tesla. Also, to provide a totally dark environment for fluorescent detection, the device was covered with opaque box. The prototype of the device with dimension 60 × 30 × 30 cm (L × W × H) and weight 10 kg is shown in Figure 5.3.

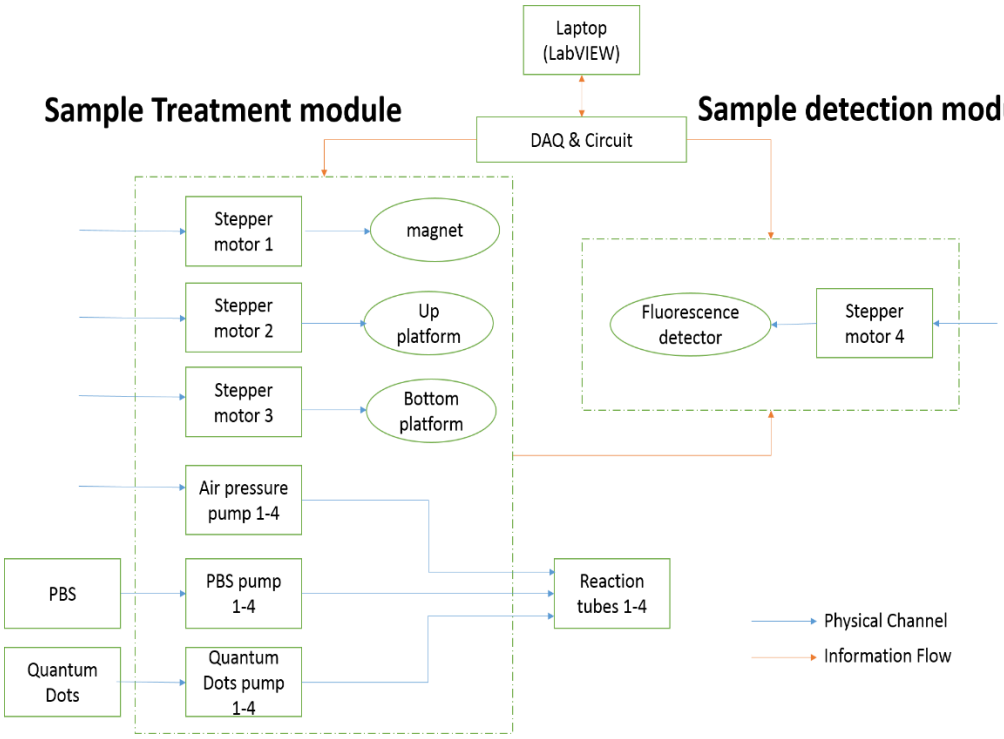

Figure 5.1 A flowchart of the biosensing system designed to separate and detect foodborne pathogenic bacteria in food samples.

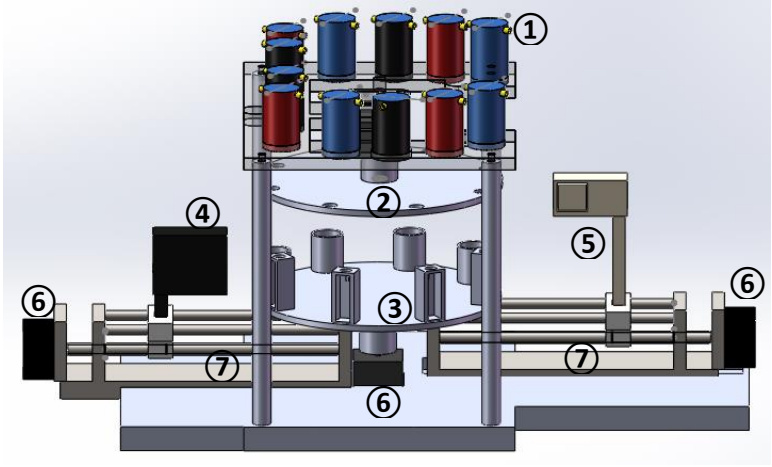

Figure 5.2 Drawing of the Mechanical device: ①Pump (Red: PBS pump, Blue: Quantum Dots Pump, Black: Air pressure Pump), ②Up platform for magnetic separation and Quantum Dots incubation (reaction tubes were not shown here), ③Bottom platform for detection and waste collection (Rectangle: sample collection for detection, cylinder: waste collection), ④Detection box for fluorescence measurement, ⑤Magnet, ⑥Stepper motor, and ⑦ Lead screw.

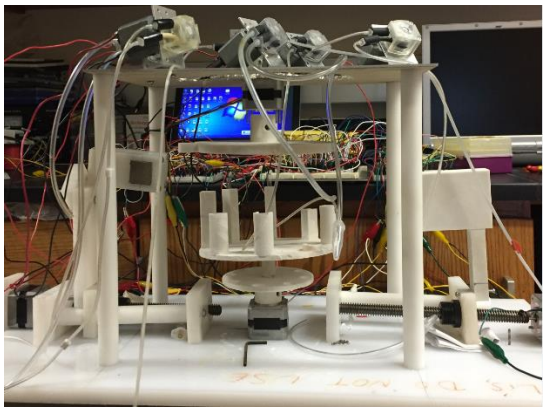

Figure 5.3 A prototype of the device with dimension 60 × 30 × 30 cm (L × W × H) and weight 10 kg.

5.3 Electronic Circuit

As shown in Figure 5.4, there were six components in electronic circuit: power supply, DAQ connector, digital I/O expansion circuit, stepper motor driver circuit, micro pump control circuit, and status indicator. And the schematic diagram of each part is shown in Figure 5.5. The circuit was designed in Protel DXP 2004 software (La jolia, CA).

In this circuit, L298N was used to build stepper motor driver circuit. IO ports of the DAQ were expanded using 74LS138 decoder and 74LS138 inverter due to the fact that there were not enough IO ports for L298N chip. Diodes in the circuit were used for protecting the L298N. With this circuit, the bipolar stepper motor could be controlled in half step or full step mode. For micro pump control circuit, 74LS138 decoder and 74LS138 inverter were used to expand IO ports and then relays were applied to control the micro pump. LEDs were used for status indicators.

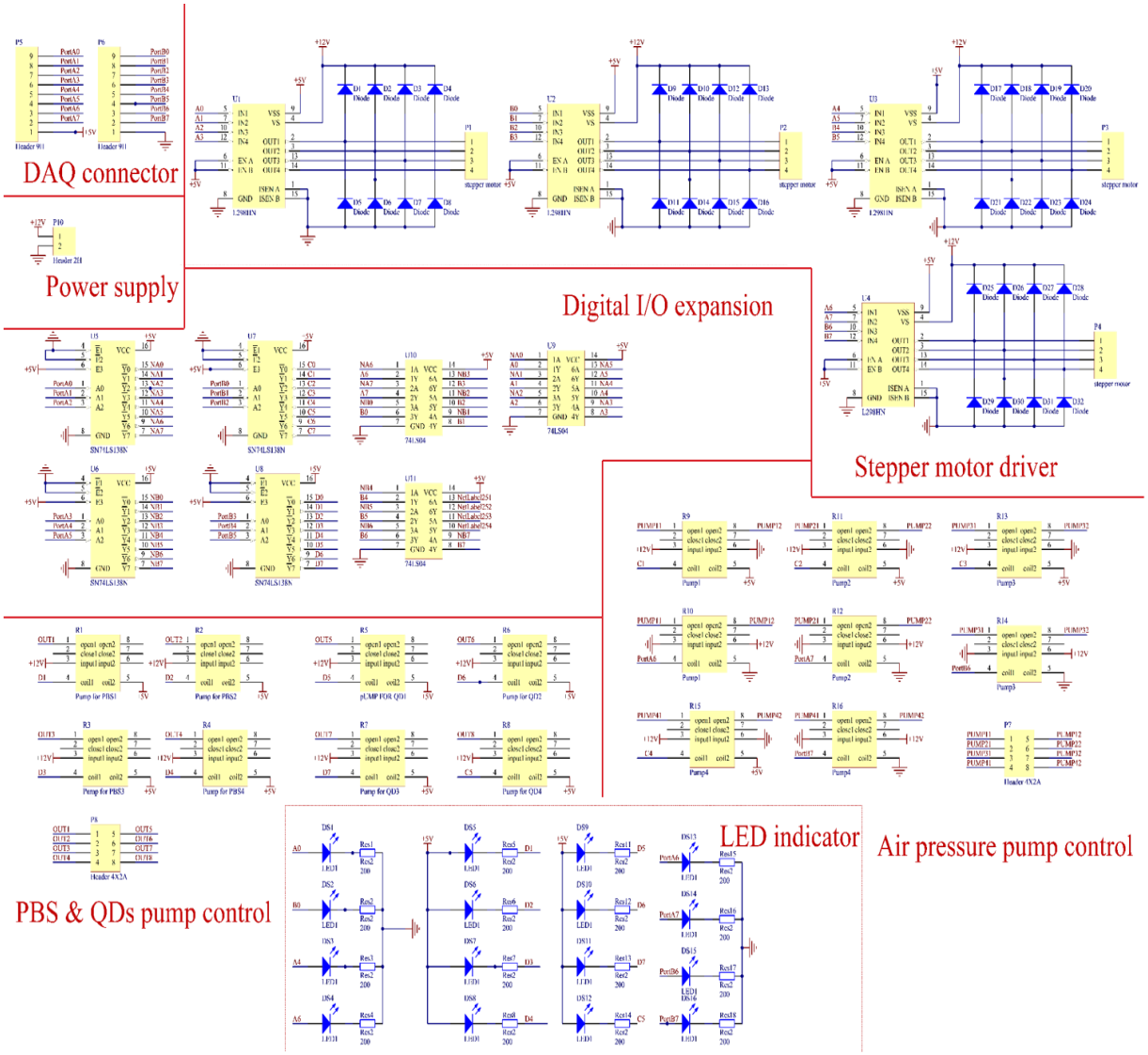

Figure 5.4 Schematic diagram of the electronic circuit.

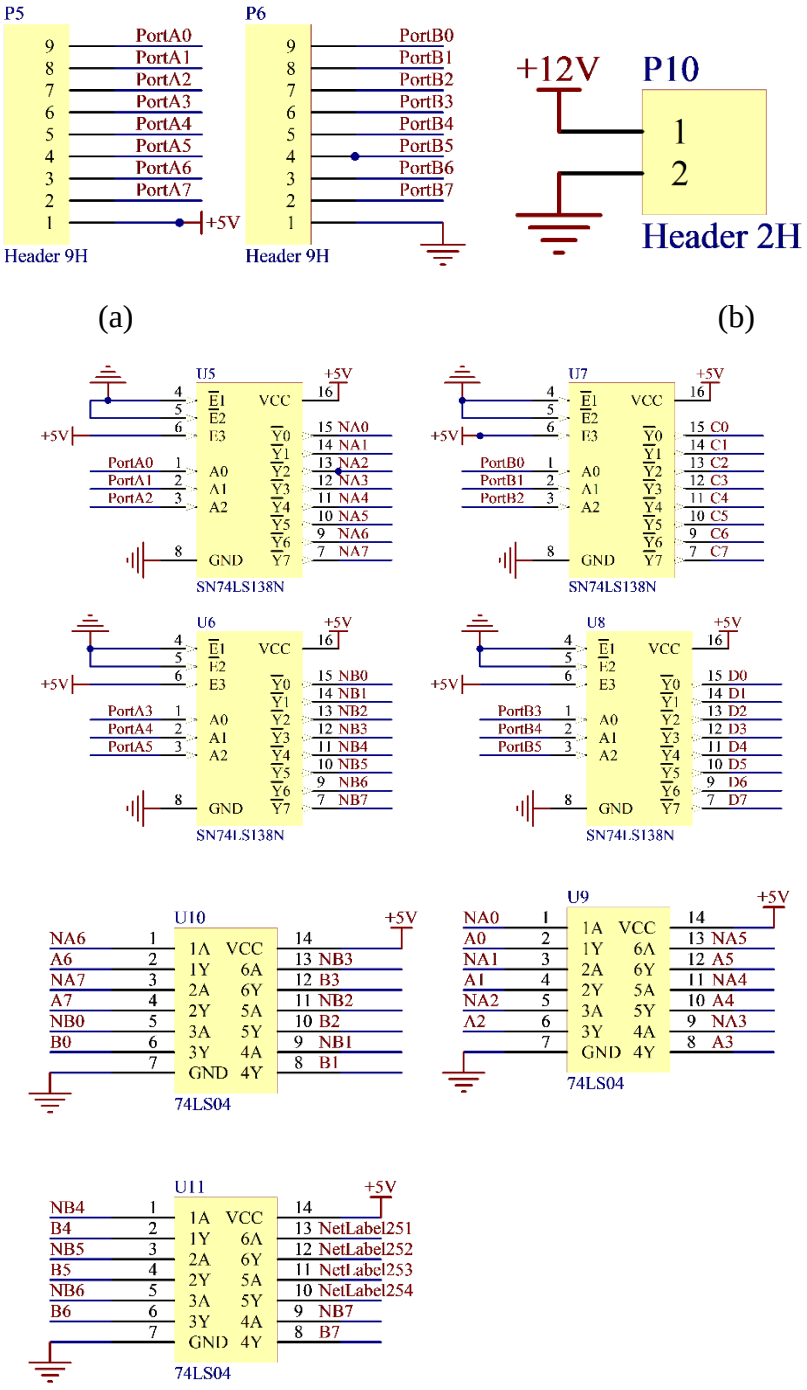

Figure 5.5 Schematic diagram of each part in the electronic circuit. (a) DAQ connector, (b) Power supply, (c) Digital I/O expansion, (d) PBS & QDs pump control, (e) Air pressure pump control, (f) stepper motor driver, and (h) LED indicator.

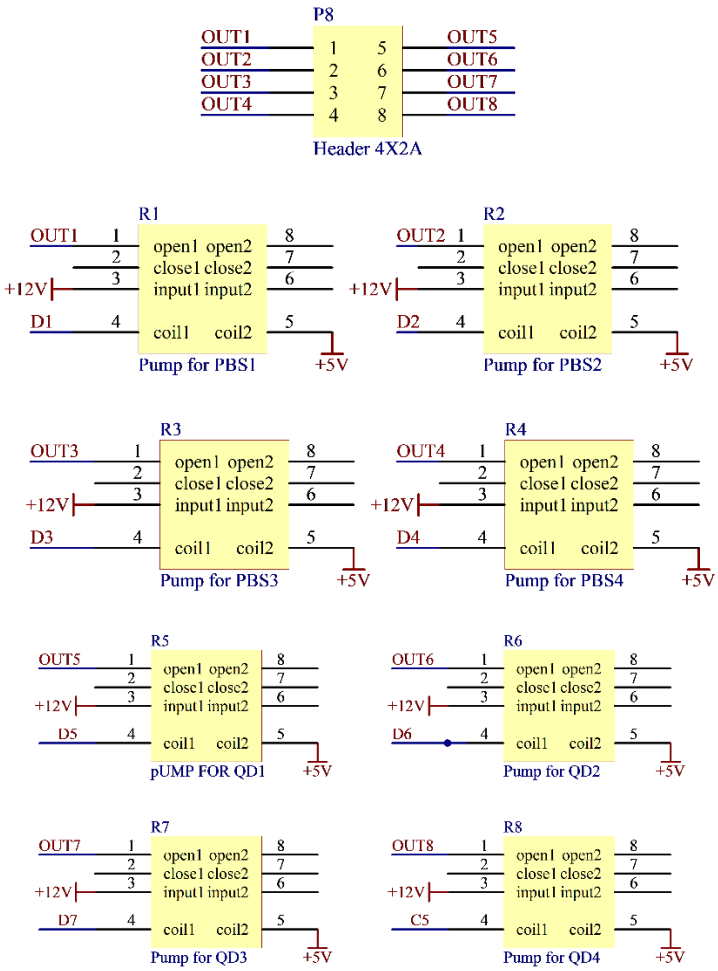

(d)

Figure 5.5 (Cont.) Schematic diagram of each part in the electronic circuit. (a) DAQ connector, (b) Power supply, (c) Digital I/O expansion, (d) PBS & QDs pump control, (e) Air pressure pump control, (f) stepper motor driver, and (h) LED indicator.

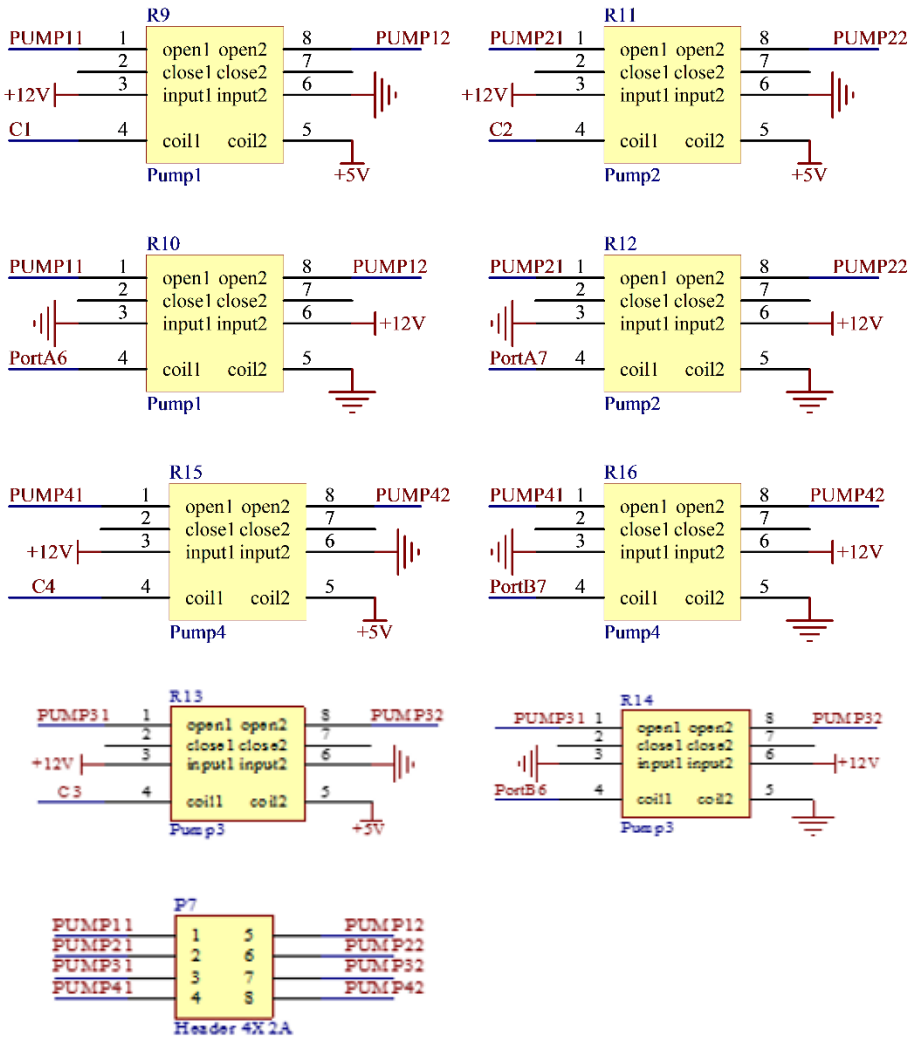

(e)

Figure 5.5 (Cont.) Schematic diagram of each part in the electronic circuit. (a) DAQ connector, (b) Power supply, (c) Digital I/O expansion, (d) PBS & QDs pump control, (e) Air pressure pump control, (f) stepper motor driver, and (h) LED indicator.

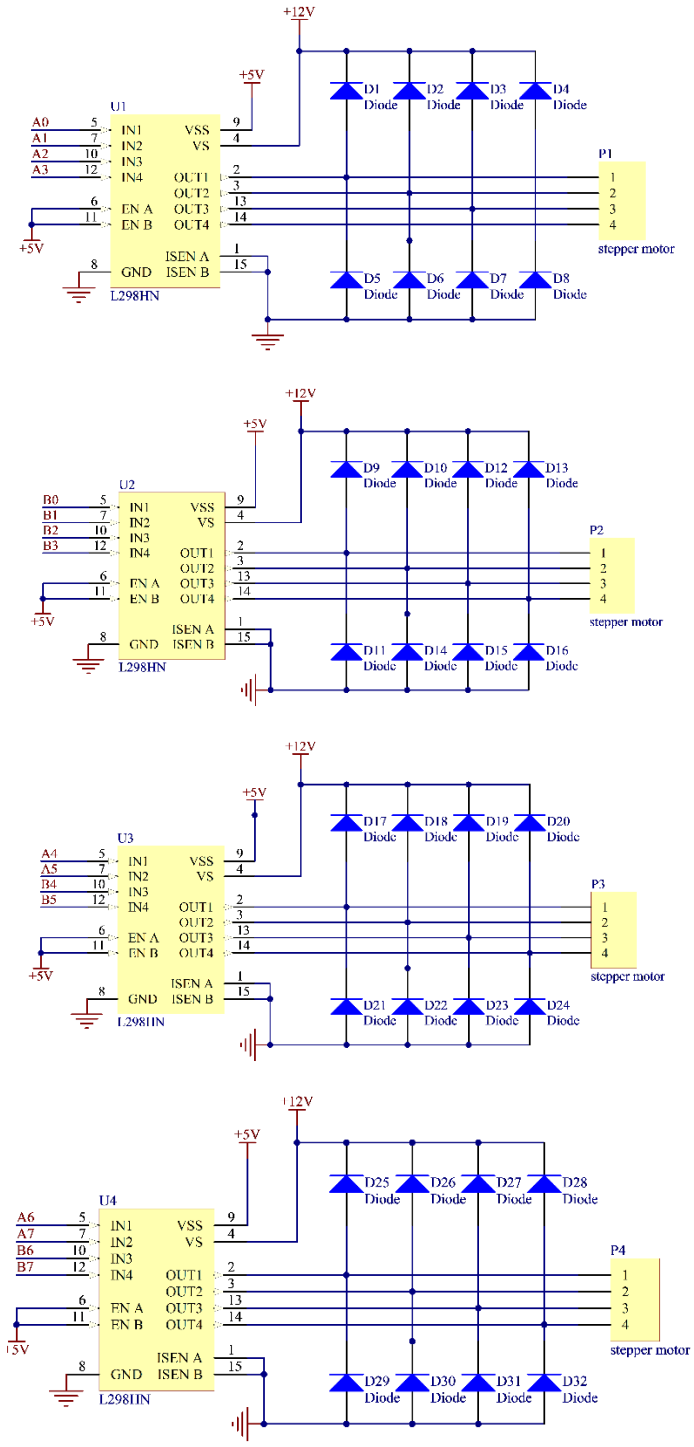

(f)

Figure 5.5 (Cont.) Schematic diagram of each part in the electronic circuit. (a) DAQ connector, (b) Power supply, (c) Digital I/O expansion, (d) PBS & QDs pump control, (e) Air pressure pump control, (f) stepper motor driver, and (h) LED indicator.

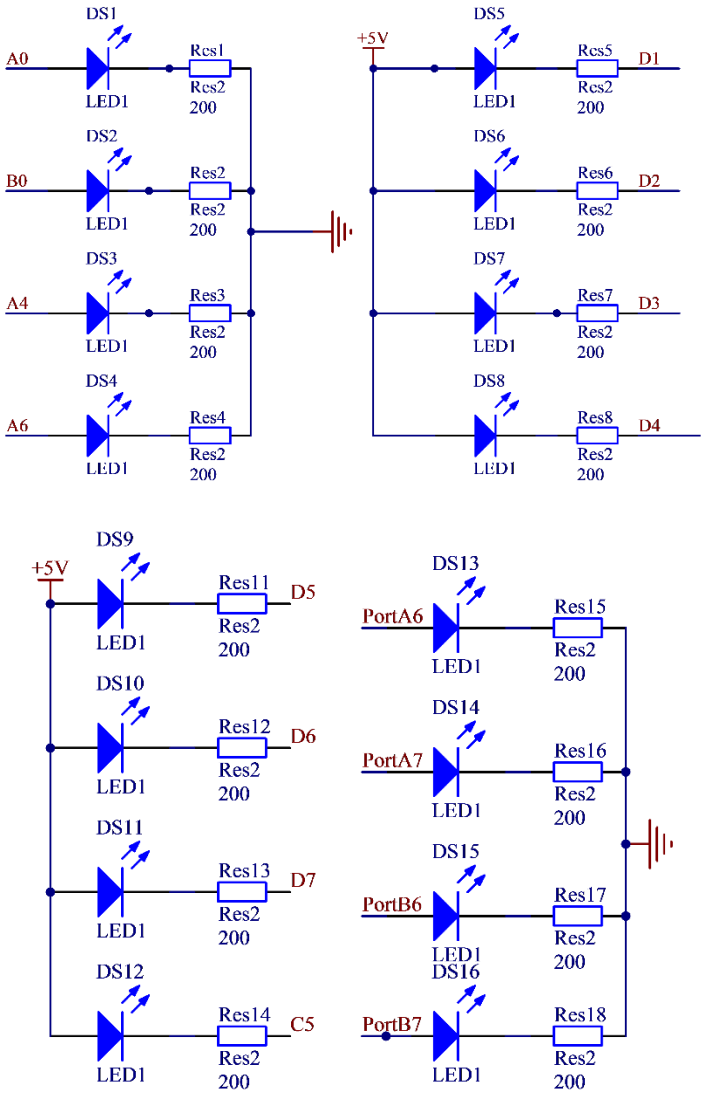

(h)

Figure 5.5 (Cont.) Schematic diagram of each part in the electronic circuit. (a) DAQ connector, (b) Power supply, (c) Digital I/O expansion, (d) PBS & QDs pump control, (e) Air pressure pump control, (f) stepper motor driver, and (h) LED indicator.

5.4 Sequential Control Software

LabVIEW (Laboratory Virtual Instrument Engineering Workbench) is a system-design platform and development environment for a visual programming language from National Instruments (Austin, TX). It can be used for building visual instruments (VIs) on a computer for measurement and control and is designed to use in almost all industry areas. Unlike the traditional programming language, LabVIEW is a graphical programming language and a typical program is written by icons instead of lines of text. LabVIEW uses dataflow programming, where the flow of data determines execution instead of instructions that determine program execution in text-based programming languages. To use LabVIEW with hardware, we need Data Acquisition to acquire data and send out orders.

LabVIEW consists of two major working interfaces for user: a block diagram and a front panel. The front panel is the user interface of the VI. Controls and indicators can be built into the front panel, which are the interactive input and output terminals of the VI, respectively. Controls include knobs, buttons, dials, and other input devices. Indicators consist of graphs, LEDs, and other displays. In the front panel, controls are used as input devices which supply data to the block diagram of the VI, while indicators are used as instrument output devices and display data acquired or generated by the block diagram.

The block diagram is the place where users can add code graphical representations of functions to control the front panel objects. Also, the terminals/icons corresponding to front panel controls and indicators will appear in the block diagram. Different icons will be connected to each other through wires. The data will flow from left to right along the wires through different icons which have certain functions.

The palettes are the tools for the programmer to use and build the block diagram and front panel. It consists of three parts: tools, controls and function palettes. Specific icons can be found for building the block diagram and front panel of VI in these palettes. Both of the front panel and the block diagram have a tool palette which is for the user to change the mouse cursor into different modes. The controls and indicators can be found in the controls palette which is available only on the front panel for the user can user to edit the front panel. The functions palette, which is available only on the block diagram, is used for editing the block diagram. It includes the Vis and functions, such as logical loops, mathematical operations, Boolean logical, file operations and signal processing. (National Instrument, 2012; Morris and Langari, 2012).

The sequential control software was programmed into the VI using LabVIEW with ULx library. Figure 5.6 shows a flowchart of all software.

The front panel was designed for users to monitor work status as shown in Figure 5.7(a). Once the system was started, the VI would automatically give instructions to the pumps and stepper motors. In the block diagram of the VI (Figure 5.7(b)), a while-loop was used to output control instructions, a formula node and five sequence structures were used for the sequential task control. The function of five sequence structures were magnetic separation with quantum dots adding, incubation timekeeping, magnetic separation after incubation, moving solution from top part to bottom part, and fluorescent detection, respectively.

Inside the sequence structure, five sub-programs, which worked for washing, half step control, full step control, air pressure control, adding PBS/QDs, were developed for control purpose and the output control signals were coded in binary format, which drove the DAQ and circuit to control the stepper motors and pumps. The sub-programs are shown in Figure 5.8. In

the software, console commands were used to control a program developed in Visual Basic for operating fluorescent measurement software and saving data into an Excel files. The name of the Excel files was the time saving data on the laptop.

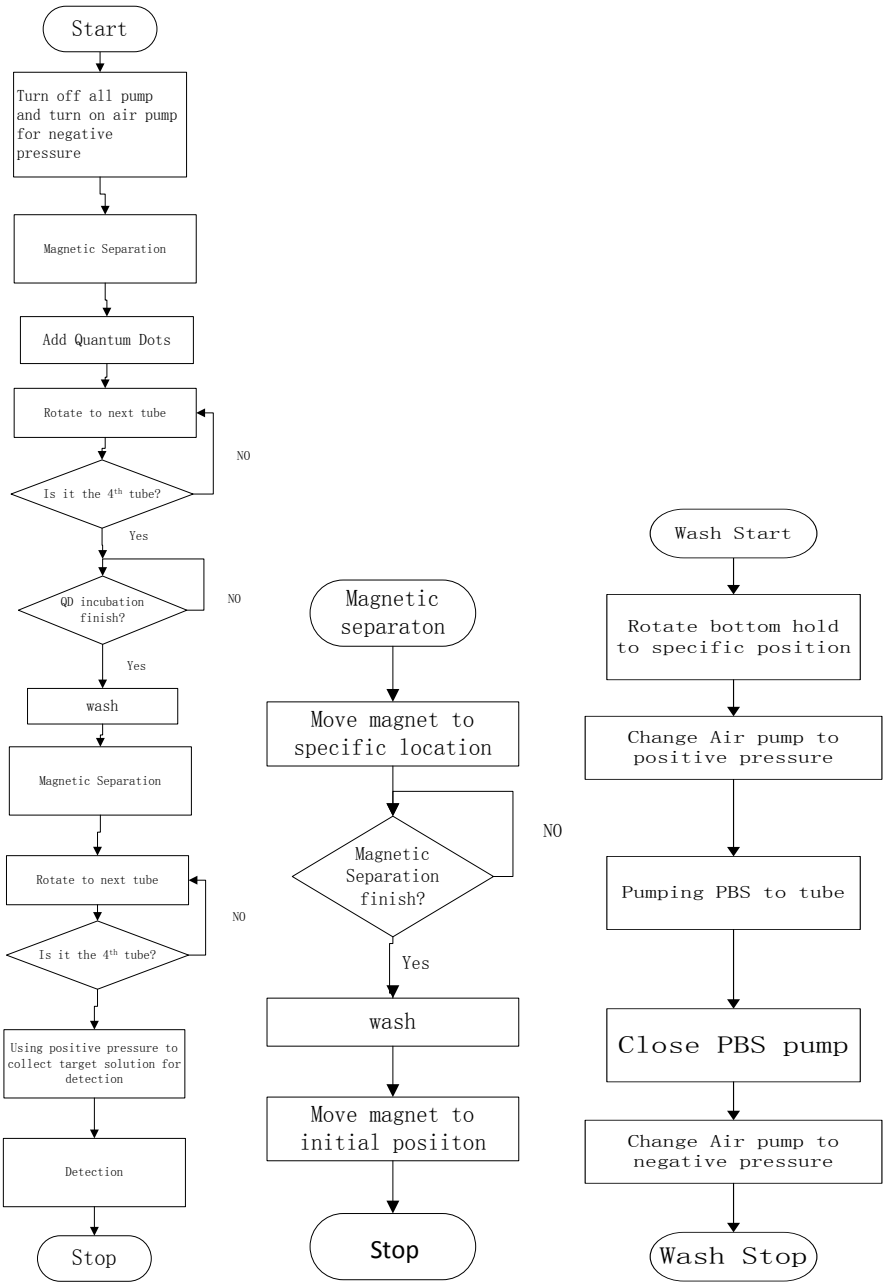

(a) (b) (c)

Figure 5.6 Flow chart of the software. (a) Main program flow chart, (b) magnetic separation sub-program flow chart, and (c) washing step sub-program flow chart.

(a)

Figure 5.7 (a) The front panel and (b) the block diagram of the virtual instrument. The front panel used for users to monitor the work status. Totally it has five sequence structures in block diagram: magnetic separation with quantum dots adding, incubation timekeeping, magnetic separation after incubation, moving solution from top part to bottom part, and fluorescent detection, respectively.

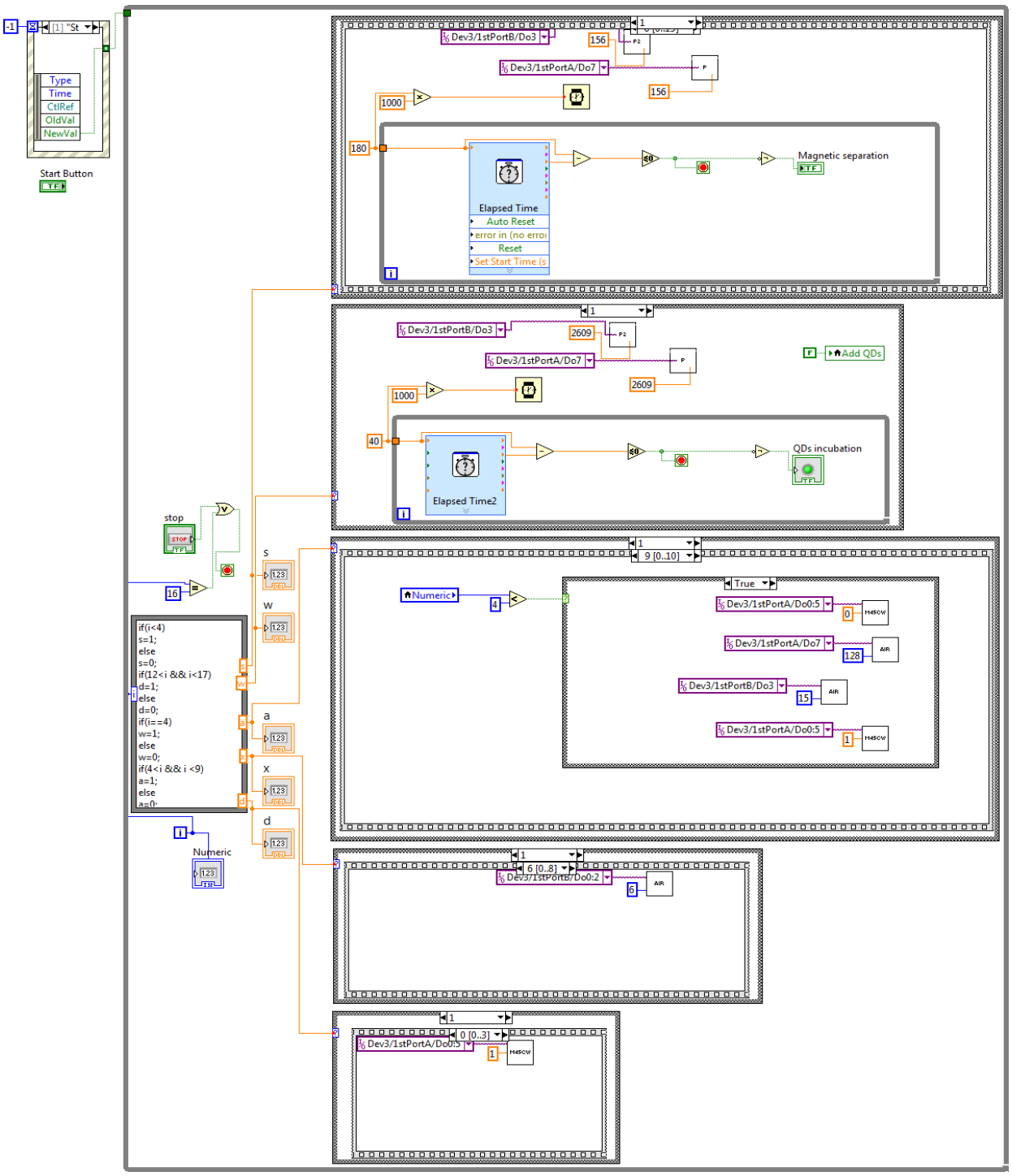

(b)

Figure 5.7 (Cont.) (a) The front panel and (b) the block diagram of the virtual instrument. The front panel used for users to monitor the work status. Totally it has five sequence structures in block diagram: magnetic separation with quantum dots adding, incubation timekeeping, magnetic separation after incubation, moving solution from top part to bottom part, and fluorescent detection, respectively.

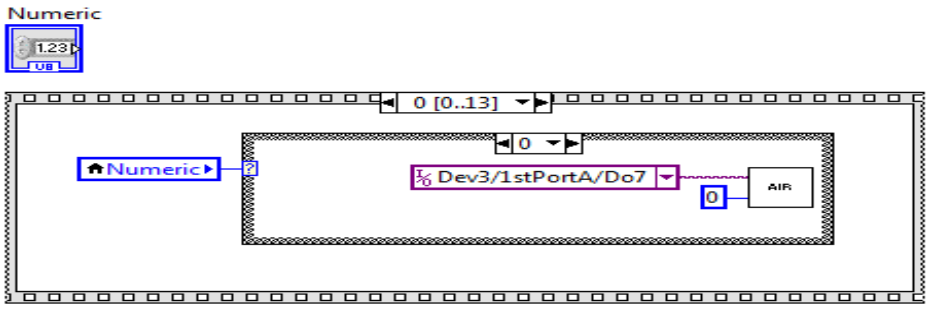

(a)

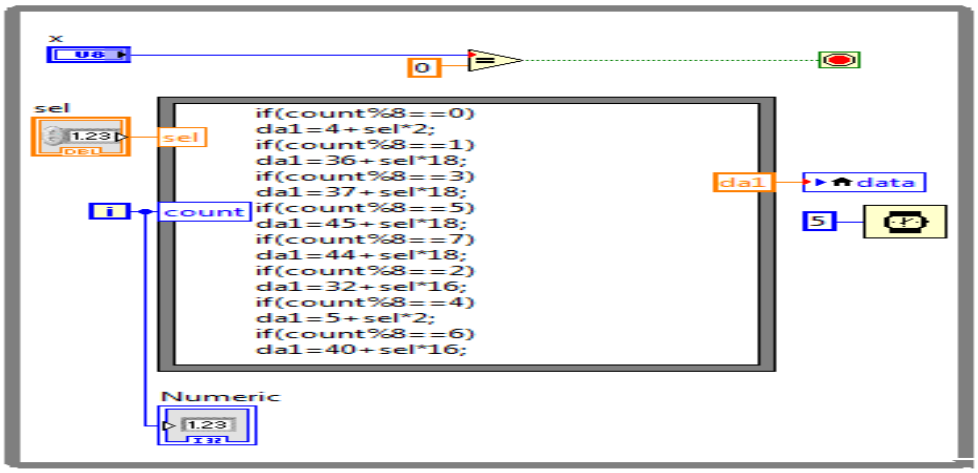

(b)

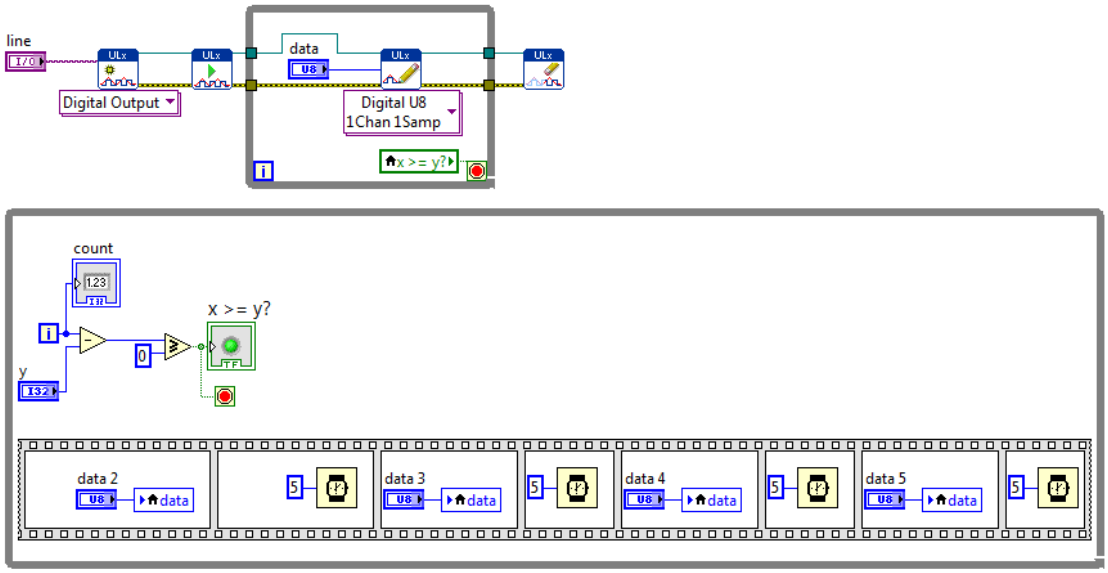

(c)

Figure 5.8 Sub-program (a) washing, (b) half step control, (c) full step control, (d) air pressure control, and (e) adding PBS/QDs.

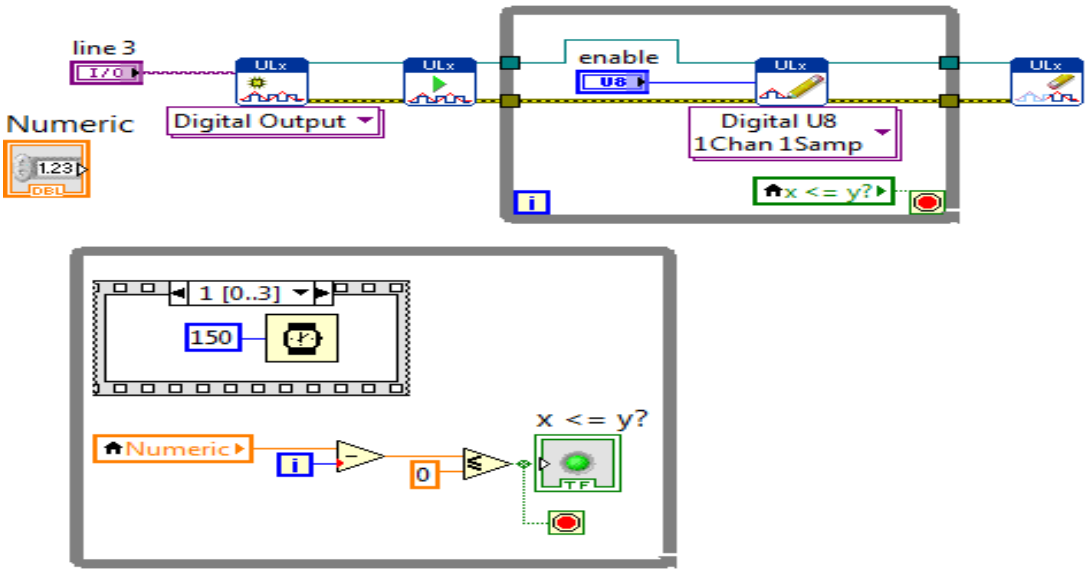

(d)

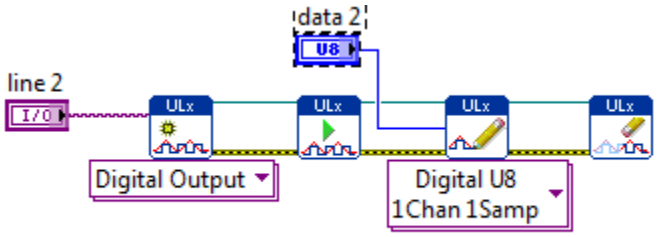

(e)

Figure 5.8 (Cont.) Sub-program (a) washing, (b) half step control, (c) full step control, (d) air pressure control, and (e) adding PBS/QDs.

5.5 Validation of the Instrument for Detection of *E. coli* O157:H7

5.5.1 Experiment Procedure for Magnetic Separation

20 µL of prepared MNB-Ab conjugates were mixed with 200 µL of the foodborne pathogen solution and then injected into the reaction tube in top platform. Another sample of the same cell dilution was placed into an empty low binding tube to use as a positive control. Then sequential control software turned on the air pressure pump to generate negative air pressure in order to

hold and mix the solution. After 40 min, the magnet in the instrument was moved to the reaction tube and then magnetic separation was done for 3 min. Once this was completed, the air pressure was changed from negative to positive to push uncaptured cells out. The uncaptured cells were collected in a new low binding tube. Then the PBS pump was turned on to do once wash step. Finally, the MNBs-cell complexes were collected in another low binding tube.

5.5.2 Experiment Procedure for Detection of *E. coli* O157:H7

20 μL of prepared MNB-Ab conjugates were mixed with foodborne pathogen solution at 4 different concentrations and then injected into reaction tubes in top platform. Run the sequential control software and finished the magnetic separation step first. The uncaptured cells were collected into the waste tube at bottom in this step. After this, corresponding air pressure was changed to negative again and the QDs pump was turned on to pump the prepared QDs-Ab conjugates into the reaction tube. For each reaction tube, a total of 200 μL of prepared QDs- Ab conjugates solution were injected. Next, the magnet was removed and rotated top platform to repeat magnet separation step, washing step and QDs injection step for other three reaction tubes. Then the sample was incubated for 40 min to form MNBs-Ab-cells-Ab-QDs sandwich structure. After incubation, magnetic separation and washing step were repeated for reaction tubes. Once washing step was completed, the PBS pumps were turned on and pumped about 200 μL of PBS into each of reaction tubes so that the sandwich complexes were resuspended in PBS solution. Then negative air pressure was applied to push solution from the reaction tube to borosilicate glass culture tube which was placed in the bottom platform, as shown in Figure 5.9. Finally, each culture tube was moved to the portable fluorescent measurement system for fluorescent measurement and the data was saved in the laptop automatically.

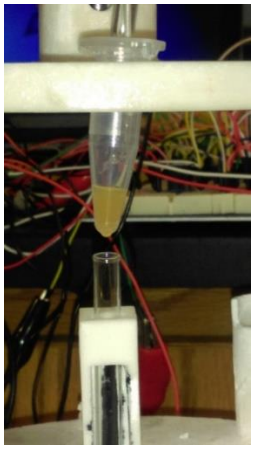

Figure 5.9 A photo of pushing test solution from the reaction tube to a glass tube.

5.5.3 Validation of Magnetic Separation Efficiency

Magnetic separeation efficiency of the biosensing system we developed needs to be validated both in pure culture and food sample.

First, the magnetic separation efficiency was validated for *E. coli* O157:H7 at 10^3 CFU/mL in pure culture solution. The results of magnetic separation efficiency are presented in Table 5.1. Based on the previous study in our lab, the magnetic separation efficiency using Ab-conjugated 150 nm MNBs for capturing *E. coli* O157:H7 was more than 90% through manual operation. Considering the sample loss in changing tubes and washing step, the results from this instrument are acceptable for further tests.

Table 5.1 The magnetic separation efficiency of *E. coli* in pure culture (10^3 CFU/mL).

Test	Separation efficiency (%)	means ± standard deviations
#1	78.2	78.3 ± 3.4 %
#2	73.9	
#3	77.8	
#4	82.2	

Then, 200 μL of ground beef wash solution inoculated with *E. coli* O157:H7 culture at 10^3 CFU/mL was used to verify the magnetic separation efficiency instead of pure culture. The results are presented in Table 5.2. Comparing with the results from pure culture, the separation efficiency was lower in ground beef sample. The possible reason was that the complex biological and chemical components in food matrix, such as proteins, fats, and carbohydrates, could interfere with the bio-recognition of antibody against target bacterium.

The standard deviation of separation efficiency was expected around 5% with more repetitive experiments in both pure culture and food samples.

Table 5.2 The result of magnetic separation efficiency of *E. coli* in ground beef wash solution (10^3 CFU/mL).

Test	**Separation efficiency (%)**	**means ± standard deviations**
#1	65.1	60.7 ± 4.2 %
#2	56.6	
#3	60.4	

5.5.4 Validation of the Specificity of Anti-*E. coli* Antibody

E. coli O157:H7 and other non-target bacteria (*Listeria monocytogenes, Salmonella* Typhimurium and *Staphylococus aureus*) at 10^6 CFU/ml were tested for validation of specificity, the results are shown in Figure 5.10. With three replicates, only the fluorescent intensity of *E. coli* O157:H7 was significantly different (P=0.002<0.05) from the negative control. There was no significant difference between negative control and *L.monocytogenes, S.*Typhimurium, *S.aureus* (P=0.23, 0.21, 0.33, respectively). This indicated that the antibody was specific to detect *E. coli*. To verify the antibody is specific to *E. coli* O157:H7, other strains of *E .coli*

should be used in specificity test. But in this reseach, the conclusion of the antibody was specific to *E. coli* was acceptable for furture experiments.

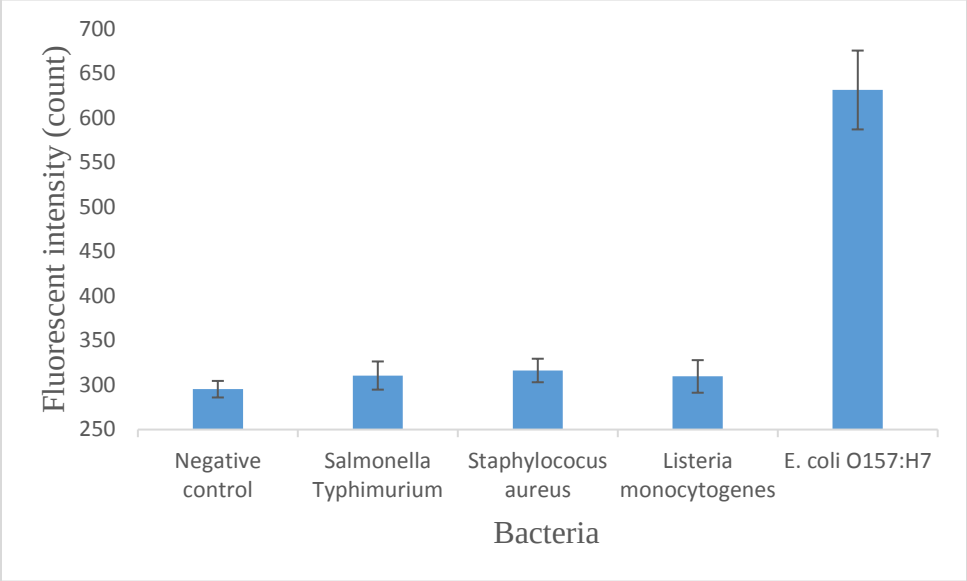

Figure 5.10 The results of specificity tests with target bacteria *E .coli* O157:H7 and non-target bacteria including *L.monocytogenes*, *S.*Typhimurium, and *S.aureus*.

5.5.5 Detection of *E. coli* O157:H7 in Pure Culture

20 µL of prepared MNBs-Ab conjugates were mixed with 600 µL of *E. coli* O157:H7 culture at different concentrations, respectively. And another 20 µL of prepared MNBs-Ab conjugates were mixed with 600 µL of PBS solution as a negative control. They were injected into reaction tubes in the top platform and then following the experiment procedure for detection of *E .coli*.

Figure 5.11 shows the typical fluorescence spectra measured for detection of *E. coli* O157:H7 at concentration ranging from 10^3 to 10^6 CFU/mL in pure culture. From the spectra, the peak was observed clearly, and the peak value increased with the increasing cell numbers. In the test, the fluorescent intensity of negative control implied that there was nonspecific binding between MNB-Ab and QD-Ab conjugates. Figure 5.12 shows a linear relationship between the

change of fluorescent intensity, which is calculated based on the difference of fluorescnet intensity between the negative control and sample soluiton at 614 nm wavelength, and the log concentration of the *E. coli*. With three replicates, the limit of detection (LOD) of the biosensing system was determined by multiplying the standard deviation of negative control measurements by 3 and was found to be 3.98×10^3 CFU/mL.

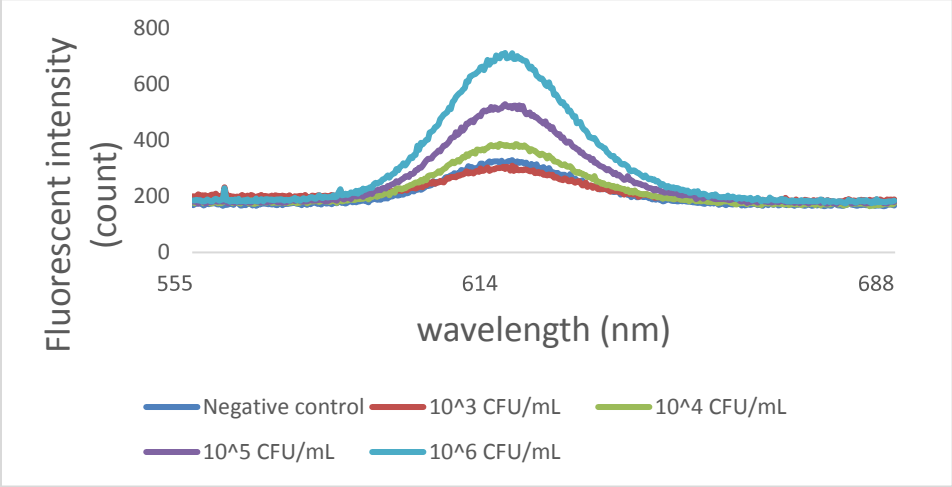

Figure 5.11 Fluorescence spectra for detection of *E. coli* O157:H7 using the biosensing system.

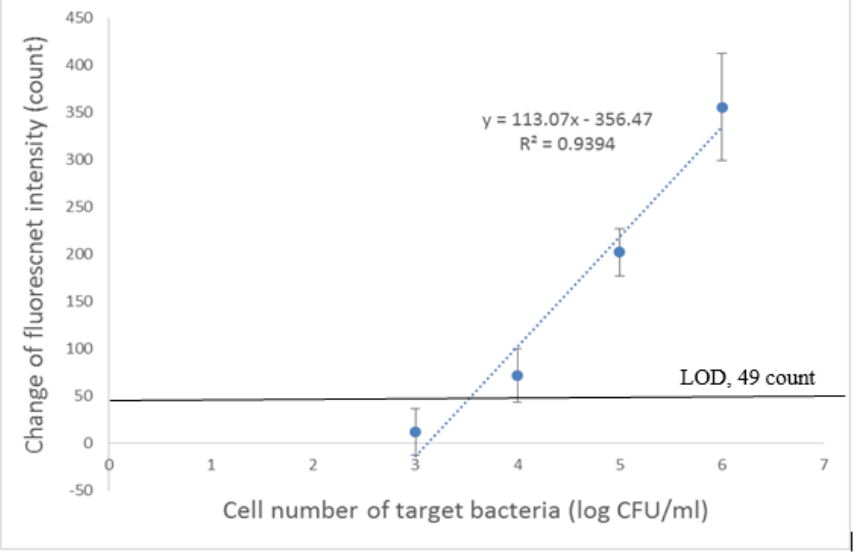

Figure 5.12 Linear relationships of the change in fluorescent intensity versus the log concentration of *E. coli* in pure culture. The limit of detection was determined by the equation based on signal/noise ratio of three, 3 × standard deviation of negative control.

5.5.6 Detection of *E. coli* O157:H7 in Ground Beef

20 µL of prepared MNBs-Ab conjugates were mixed with 600 µL of prepared ground beef wash solution inoculating with *E. coli* O157:H7 at different concentrations, respectively. And another 20 µL of prepared MNBs-Ab conjugates were mixed with 600 µL of prepared ground beef wash solution without *E. coli* O157:H7 as a negative control. They were injected into the reaction tubes in the top platform and then following the experiment process.

Figure 5.13 shows the typical fluorescence spectra measured for detection of *E. coli* O157:H7 at concentration ranging from 10^3 to 10^6 CFU/mL in ground beef samples. Figure 5.14 shows a linear relationship between the change of fluorescent intensity and the log concentration of the *E. coli*. The limit of detection (LOD) was calculated similarly and was found to be 6.46×10^4 CFU/mL.

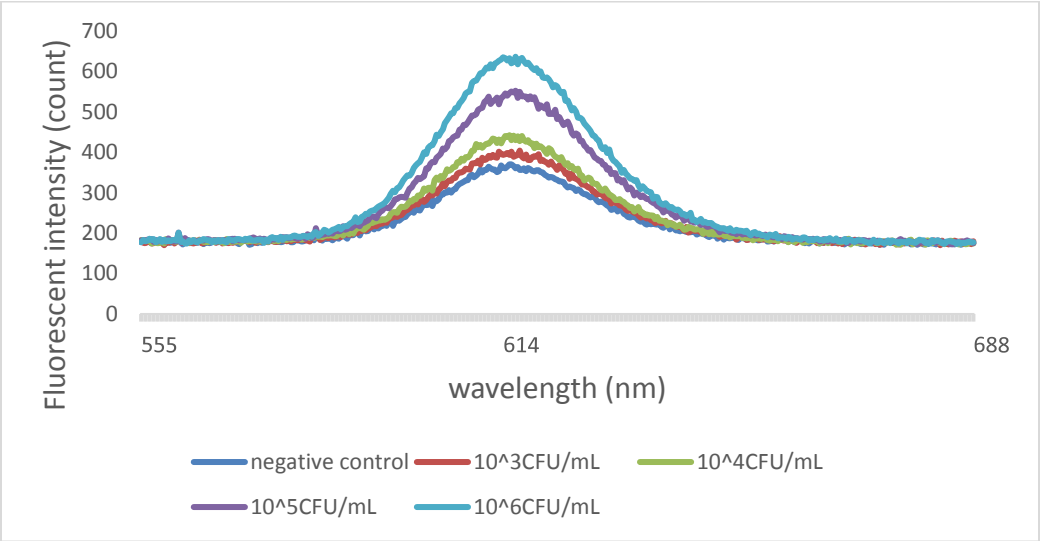

Figure 5.13 Fluorescence spectra for detection of *E. coli* O157:H7 in ground beef samples using the biosensing system.

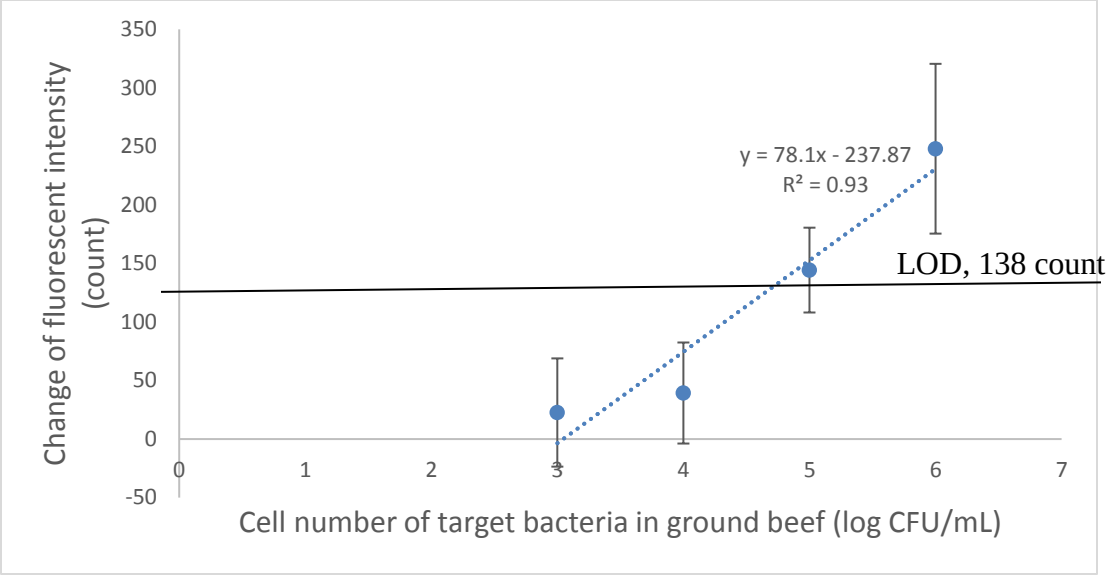

Figure 5.14 Linear relationships of the change in fluorescent intensity versus the log concentration of *E. coli* in ground beef samples. The limit of detection was determined by the equation based on signal/noise ratio of three, 3 × standard deviation of negative control.

5.6 Comparisons of the Developed Biosensing Instrument with Manual Operation, Some Commercial Products and Research Prototypes

Comparing the results reported by Wang *et al.* (2011) and Xu *et al.* (2015) through manual operation using the similar method, the LOD was higher in the biosensor system developed in this study. The possible reasons were that 10-15% of the QD-Ab conjugates solution could be lost when the solution was pumped into the reaction tube as shown in Table 5.3, and still small quantity of the sample solution was left in the reaction tube when they were pushed from top to bottom for detection due to the rough edge of the hole in the bottom of the reaction tube. And also , the lower separation efficiency in the system was another possible reason for higher LOD.

Table 5.3 The results of tests on quantum dot solution loss in tubing (10 mL of quantum dots mixed with 190 mL of PBS solution).

Test	Fluorescent intensity before solution pass through the tubing (count)	Fluorescent intensity after solution pass through the tubing (count)	Difference (%)
#1	4193	3648	13.0
#2	4150	3528	15.0
#3	4214	3750	11.1

Comparing with some commercial products and prototypes from other researchers, as shown in Table 5.4, the biosesing instrument we developed was still promising. The major advantage of this instrument was that it could automatically finish the separation function and detection function in one instrument for four samples in 2 hours. These helped reduce the detection time and labor intensiveness. But the LOD was still higher than comercial product and peer work.

Table 5.4 Comparison of biosensing instrument we developed with some commercial products and research prototypes.

Instrument	Target	Target isolation	Detection time	Limit of detection	Reference
Impedance based biosensing instrument with flowcell	H5N1 virus	Not Available	105 min for one sample	0.84 HAU per 200 μL in pure culture	Callaway *et al.*, 2016
Quantum dot based nano-biosensor system (need manual operation to put captured bacteria into detector)	*Salmonella*	Magnetic separation method.	70 min for one sample	10^3 CFU/mL in pure culture	Kim *et al.*, 2015
PR610-2 instrument	*E .coli* O157:H7	Not Available	15 min for detecting one prepared sample.	10^2 CFU/mL	Research International, Inc.
Aegis 1000 instrument	Bacteria, biomarkers	Use capillary to capture target agents	60 min for one bacteria sample. 30 min for one biomarker sample	10^3 CFU/mL for bacteria pg/mL range for biomarker	Biodetection Instruments, LLC.
Biosensing instrument developed in this research	*E .coli* O157:H7	Magnetic separation method.	120 min for four samples	3.98×10^3 and 6.46×10^4 CFU/mL in pure culture and ground beef samples	This thesis

Chapter 6 Conclusions and Recommendations

A prototype of the portable biosensing instrument was designed and fabricated for separation and detection of foodborne pathogens using nanobead-based magnetic separation and quantum dot-labeled fluorescent measurement. *E. coli* O157:H7 was used as a model pathogen in this study. The instrument could be controlled by the virtual instrument developed in LabVIEW to conduct magnetic separation, washing, add quantum dots, incubation, data processing and storage automatically. The magnetic separation efficiency of this instrument was 78.3 ± 3.4% and 60.7 ± 4.2% for *E. coli* O157:H7 in pure culture and ground beef samples, respectively. The limit of detection for *E. coli* O157:H7 was 3.98×10^3 and 6.46×10^4 CFU/mL in pure culture and ground beef samples, respectively. The detection could be finished in 2 hours for samples simultaneously. It showed great potential to be applied to the in-field detection of foodborne pathogens in agriculture and food.

Further work on this study could concentrate on the improvement of sensitivity. This could be done with the following approaches:

1. Improve the mechanical precision of the whole device so that the solution could be pushed from top to bottom easier and more stable.
2. Optimize the position of pumps to reduce the length of tubing for minimizing the loss of quantum dots-antibody conjugates in solution.
3. Optimize the volumes of nanobeads, antibodies, quantum dots, and sample solution need to be used for each test to minimize the cost.
4. Optimize the magnetic separation time to reduce the chance of aggregation of magnetic nanobeads.

References

Abdelhamid, H. N., & Wu, H. F. (2013). Probing the interactions of chitosan capped CdS quantum dots with pathogenic bacteria and their biosensing application. *Journal of Materials Chemistry B, 1*(44), 6094-6106.

Algar, W. R., Tavares, A. J., & Krull, U. J. (2010). Beyond labels: A review of the application of quantum dots as integrated components of assays, bioprobes, and biosensors utilizing optical transduction. *Analytica Chimica Acta,* 673(1), 1-25.

Arora, P., Sindhu, A., Dilbaghi, N., & Chaudhury, A. (2011). Biosensors as innovative tools for the detection of food borne pathogens. *Biosensors and Bioelectronics,* 28(1), 1-12.

Ashoori, R. (1996). Electrons in artificial atoms. *Nature,* 379, 413-419.

Ballarini, A., Segata, N., Huttenhower, C., & Jousson, O. (2013). Simultaneous quantification of multiple bacteria by the BactoChip microarray designed to target species-specific marker genes. *PloS One,* 8(2), e55764.

Bennett, A., MacPhee, S., & Betts, R. (1996). The isolation and detection of *Escherichia coli* O157 by use of immunomagnetic separation and immunoassay procedures. *Letters in Applied Microbiology,* 22(3), 237-243.

Besser, MD, Richard E., Patricia M. Griffin, MD, and Laurence Slutsker, MD, MPH. (1999). *Escherichia coli* O157: H7 gastroenteritis and the hemolytic uremic syndrome: an emerging infectious disease 1. *Annual Review of Medicine,* 50.1: 355-367.

Bettiol, A. A., Van Kan, J., Sum, T., & Watt, F. (2001). A LabVIEW™-based scanning and control system for proton beam micromachining. *Nuclear Instruments and Methods in Physics Research Section B: Beam Interactions with Materials and Atoms,* 181(1), 49-53.

Bhardwaj, T. (2015). Review on biosensor technologies. *International Journal of Advanced Research in Engineering and Technology,* 6(2), 36-62.

Biodetection Instruments. Retrieved from http://biodetection-instruments.com/products.html. Accessed in November, 2016.

Brandão, D., Liébana, S., Campoy, S., Alegret, S., & Pividori, M. I. (2015). Immunomagnetic separation of *Salmonella* with tailored magnetic micro and nanocarriers. A comparative study. *Talanta, 143, 198-204.*

Bunde, R. L., Jarvi, E. J., & Rosentreter, J. J. (1998). Piezoelectric quartz crystal biosensors. *Talanta, 46(6), 1223-1236.*

Callaway, Z., Wang, Y., Zhang, B., Zhang, T., Costello, T. A., Slavik, M. F., & Li, Y. (2016). A portable impedance biosensing system for rapid detection of avian influenza virus. *Transactions of the ASABE,* 59(2): 421-428.

Carrillo-Carrión, C., Simonet, B. M., & Valcárcel, M. (2011). Colistin-functionalised CdSe/ZnS quantum dots as fluorescent probe for the rapid detection of *Escherichia coli*. *Biosensors and Bioelectronics*, *26*(11), 4368-4374.

CDC (Centers for Disease Control and Prevention). (2016). *List of selected multistate foodborne outbreak investigations*, http://www.cdc.gov/foodsafety/outbreaks/multistate-outbreaks/outbreaks-list.html. Assessed in November 2016.

Chan, K. Y., Ye, W. W., Zhang, Y., Xiao, L. D., Leung, P. H., Li, Y., & Yang, M. (2013). Ultrasensitive detection of E. coli O157: H7 with biofunctional magnetic bead concentration via nanoporous membrane based electrochemical immunosensor. *Biosensors and Bioelectronics*, *41*, 532-537.

Chandler, D. P., Brown, J., Call, D. R., Wunschel, S., Grate, J. W., Holman, D. A., Bruckner-Lea, C. J. (2001). Automated immunomagnetic separation and microarray detection of *E. coli* O157: H7 from poultry carcass rinse. *International Journal of Food Microbiology,* 70(1), 143-154.

Chen, X., Gan, M., Xu, H., Chen, F., Ming, X., Xu, H., & Liu, C. (2014). Development of a rapid and sensitive quantum dot-based immunochromatographic strip by double labeling PCR products for detection of Staphylococcus aureus in food. *Food Control*, *46*, 225-232.

Chidawanyika, W., Litwinski, C., Antunes, E., & Nyokong, T. (2010). Photophysical study of a covalently linked quantum dot–low symmetry phthalocyanine conjugate. *Journal of Photochemistry and Photobiology A: Chemistry*, 212(1), 27-35.

Collier, C., Vossmeyer, T., & Heath, J. (1998). Nanocrystal superlattices. *Annual Review of Physical Chemistry*, 49(1), 371-404.

de Boer, E., & Beumer, R. R. (1999). Methodology for detection and typing of foodborne microorganisms. *International Journal of Food Microbiology,* 50(1), 119-130.

Dogan, Ü, Kasap, E., Cetin, D., Suludere, Z., Boyaci, I. H., Türkyılmaz, C., Tamer, U. (2016). Rapid detection of bacteria based on homogenous immunoassay using chitosan modified quantum dots. *Sensors and Actuators B: Chemical,* 233, 369-378.

Don Whitley Scientific Ltd. Retrieved from http://www.dwscientific.co.uk/rabit/. Accessed in November, 2016.

Duan, N., Wu, S., Yu, Y., Ma, X., Xia, Y., Chen, X., & Wang, Z. (2013). A dual-color flow cytometry protocol for the simultaneous detection of Vibrio parahaemolyticus and

Salmonella typhimurium using aptamer conjugated quantum dots as labels. *Analytica Chimica Acta, 804*, 151-158.

Duplan, V., Frost, E., & Dubowski, J. J. (2011). A photoluminescence-based quantum semiconductor biosensor for rapid in situ detection of Escherichia coli. *Sensors and Actuators B: Chemical*, *160*(1), 46-51.

Ekimov, A. I., & Onushchenko, A. A. (1981). Quantum size effect in three-dimensional microscopic semiconductor crystals. *ZhETF Pisma Redaktsiiu*, 34, 363.

Elliott, C., Vijayakumar, V., Zink, W., & Hansen, R. (2007). National instruments LabVIEW: A programming environment for laboratory automation and measurement. *Journal of the Association for Laboratory Automation*,12(1), 17-24.

Fan, X., White, I. M., Shopova, S. I., Zhu, H., Suter, J. D., & Sun, Y. (2008). Sensitive optical biosensors for unlabeled targets: A review. *Analytica Chimica Acta*, 620(1), 8-26.

Fernandez, T. F. (2008). *E. coli* O157: H7. *Veterinary World* 1.3: 83-87.

Foudeh, A. M., Didar, T. F., Veres, T., & Tabrizian, M. (2012). Microfluidic designs and techniques using lab-on-a-chip devices for pathogen detection for point-of-care diagnostics. *Lab on a Chip*, 12(18), 3249-3266.

Frasco, M. F., & Chaniotakis, N. (2009). Semiconductor quantum dots in chemical sensors and biosensors. *Sensors*, 9(9), 7266-7286.

He, J., Huang, M., Wang, D., Zhang, Z., & Li, G. (2014). Magnetic separation techniques in sample preparation for biological analysis: A review. *Journal of Pharmaceutical and Biomedical Analysis*, 101, 84-101.

Hu, Y., Wang, C., Bai, B., Li, M., Wang, R., & Li, Y. (2014). Detection of *Staphylococcus aureus* using quantum dots as fluorescence labels. *International Journal of Agricultural and Biological Engineering*, 7(1), 77.

Hsing, I., Xu, Y., & Zhao, W. (2007). Micro-and Nano-Magnetic particles for applications in biosensing. *Electroanalysis*, 19(7-8), 755-768.

Ikanovic, M., Rudzinski, W. E., Bruno, J. G., Allman, A., Carrillo, M. P., Dwarakanath, S., & Andrews, C. J. (2007). Fluorescence assay based on aptamer-quantum dot binding to Bacillus thuringiensis spores. *Journal of Fluorescence*, *17*(2), 193-199.

IUPAC. (1997). Compendium of Chemical Terminology, 2nd ed. (the "Gold Book"). Compiled by A. D. McNaught and A. Wilkinson. Blackwell Scientific Publications, Oxford. XML on-line corrected version: http://goldbook.iupac.org created by M. Nic, J. Jirat, B. Kosata; updates compiled by A. Jenkins. ISBN 0-9678550-9-8.

Jin, H., Lin, J., Wang, X., Xin, T., Liang, S., Li, Z., & Hu, G. (2009). Magnetic particle-based chemiluminescence enzyme immunoassay for free thyroxine in human serum. *Journal of Pharmaceutical and Biomedical Analysis,*50(5), 891-896.

Joo, J., Yim, C., Kwon, D., Lee, J., Shin, H. H., Cha, H. J., & Jeon, S. (2012). A facile and sensitive detection of pathogenic bacteria using magnetic nanoparticles and optical nanocrystal probes. *Analyst, 137*(16), 3609-3612.

Kanayeva, D. A., Wang, R., Rhoads, D., Erf, G. F., Slavik, M. F., Tung, S., & Li, Y. (2012). Efficient separation and sensitive detection of Listeria monocytogenes using an impedance immunosensor based on magnetic nanoparticles, a microfluidic chip, and an interdigitated microelectrode. *Journal of Food Protection*, *75*(11), 1951-1959.

Kasfner, M. A. (1993). Artificial atoms. *Physics Today*, 46, 24-31.

Kim, G., Moon, J., Moh, C., & Lim, J. (2015). A microfluidic nano-biosensor for the detection of pathogenic *Salmonella*. *Biosensors and Bioelectronics*, 67, 243-247.

Kim, N., Kang, H., Jang, Y., Ryoo, S., Lee, H., Shin, S. J., Park, Y. H. (2016). Comparison of two immunomagnetic separation methods for detection of *Mycobacterium avium* subsp. paratuberculosis in bovine feces. *International Journal of Applied Research in Veterinary Medicine,* 14(1), 96-104.

Kuang, H., Cui, G., Chen, X., Yin, H., Yong, Q., Xu, L., & Xu, C. (2013). A one-step homogeneous sandwich immunosensor for Salmonella detection based on magnetic nanoparticles (MNPs) and quantum dots (QDs). *International journal of molecular sciences*, *14*(4), 8603-8610.

Kwon, D., Lee, S., Ahn, M. M., Kang, I. S., Park, K. H., & Jeon, S. (2015). Colorimetric detection of pathogenic bacteria using platinum-coated magnetic nanoparticle clusters and magnetophoretic chromatography. *Analytica Chimica Acta*, 883, 61-66.

Law, J. W., Ab Mutalib, N., Chan, K., & Lee, L. (2015). Rapid methods for the detection of foodborne bacterial pathogens: Principles, applications, advantages and limitations. *Frontiers in Microbiology*, 5, 770.

Lazcka, O., Del Campo, F. J., & Munoz, F. X. (2007). Pathogen detection: A perspective of traditional methods and biosensors. *Biosensors and Bioelectronics,* 22(7), 1205-1217.

Lee, H., Yoon, T., & Weissleder, R. (2009). Ultrasensitive detection of bacteria using Core–Shell nanoparticles and an NMR-Filter system. *Angewandte Chemie International Edition,* 48(31), 5657-5660.

Li, Yanbin. (2006). Section 2.3 Biosensors, pp. 52-93, of Chapter 2 Hardware, in CIGR Handbook of Agricultural Engineering Volume VI Information Technology. USA: ASABE.

Li, M., Li, Y., Chen, Q & Lin, J. (2015). A high gradient and strength bioseparator with nano-sized immunomagnetic particles for specific separation and efficient concentration of *E. coli* O157: H7. *Journal of Magnetism and Magnetic Materials*, 378, 206-213.

Liang, W., Liu, S., Song, J., Hao, C., Wang, L., Li, D., & He, Y. (2015). Highly sensitive fluorescence biosensors for sparfloxacin detection at nanogram level based on electron transfer mechanism of cadmium telluride quantum dots. *Biotechnology Letters*, 37(5), 1057-1061.

Luo, Y., Nartker, S., Wiederoder, M., Miller, H., Hochhalter, D., Drzal, L. T., & Alocilja, E. C. (2012). Novel biosensor based on electrospun nanofiber and magnetic nanoparticles for the detection of E. coli O157: H7. *IEEE Transactions on Nanotechnology*, *11*(4), 676-681.

Malorny, B., Tassios, P. T., Rådström, P., Cook, N., Wagner, M., & Hoorfar, J. (2003). Standardization of diagnostic PCR for the detection of foodborne pathogens. *International Journal of Food Microbiology*, 83(1), 39-48.

Mandal, P., Biswas, A., Choi, K., & Pal, U. (2011). Methods for rapid detection of foodborne pathogens: An overview. *American Journal of Food Technology*, 6(2), 87-102.

Martelet, A., L'Hostis, G., Nevers, M., Volland, H., Junot, C., Becher, F., & Muller, B. H. (2015). Phage amplification and immunomagnetic separation combined with targeted mass spectrometry for sensitive detection of viable bacteria in complex food matrices. *Analytical Chemistry*, 87(11), 5553-5560.

Mead, Paul S., and Patricia M. Griffin. (1998). *Escherichia coli* O157: H7. *The Lancet* 352.9135*:* 1207-1212.

Mohanty, S. P., & Kougianos, E. (2006). Biosensors: A tutorial review. *IEEE Potentials*, 25(2), 35-40.

Morris, A. S., & Langari, R. (2012). Measurement and Instrumentation: Theory and Application. Academic Press, Salt Lake City, UT.

Mukhopadhyay, B., Martins, M. B., Karamanska, R., Russell, D. A., & Field, R. A. (2009). Bacterial detection using carbohydrate-functionalised CdS quantum dots: a model study exploiting E. coli recognition of mannosides. *Tetrahedron Letters*, *50*(8), 886-889.

National Instruments. (2012). LabVIEW User Manual. Austin, TX.

Nikitin, P. V., & Rao, K. S. (2009). LabVIEW-based UHF RFID tag test and measurement system. *IEEE Transactions on Industrial Electronics*, 56(7), 2374-2381.

Omiccioli, E., Amagliani, G., Brandi, G., & Magnani, M. (2009). A new platform for real-time PCR detection of *Salmonella* spp., *Listeria* monocytogenes and *Escherichia coli* O157 in milk. *Food Microbiology*, 26(6), 615-622.

Øren, A., Husebø, C., Iversen, A., & Austgulen, R. (2005). A comparative study of immunomagnetic methods used for separation of human natural killer cells from peripheral blood. *Journal of Immunological Methods,* 303(1), 1-10.

Ozkan, M. (2004). Quantum dots and other nanoparticles: What can they offer to drug discovery? *Drug Discovery Today,* 9(24), 1065-1071.

Qiu, J., Zhou, Y., Chen, H., & Lin, J. (2009). Immunomagnetic separation and rapid detection of bacteria using bioluminescence and microfluidics. *Talanta,* 79(3), 787-795.

Resch-Genger, U., Grabolle, M., Cavaliere-Jaricot, S., Nitschke, R., & Nann, T. (2008). Quantum dots versus organic dyes as fluorescent labels. *Nature Methods,* 5(9), 763-775.

Research International, Inc. Retrieved from http://www.resrchintl.com/PR610-2_Food_Safety_Testing.html. Accessed in November, 2016.

Romero, M. R., D'Agostino, M., Arias, A. P., Robles, S., Casado, C. F., Iturbe, L. O., Cook, N. (2016). An immunomagnetic separation/loop-mediated isothermal amplification method for rapid direct detection of thermotolerant *Campylobacter* spp. during poultry production. *Journal of Applied Microbiology,* 120(2), 469-477.

Rusling, J. F., Kumar, C. V., Gutkind, J. S., & Patel, V. (2010). Measurement of biomarker proteins for point-of-care early detection and monitoring of cancer. *Analyst,* 135(10), 2496-2511.

Salehi, D., & Brandt, M. (2006). Melt pool temperature control using LabVIEW in Nd: YAG laser blown powder cladding process. *International Journal of Advanced Manufacturing Technology,* 29(3-4), 273-278.

Sanvicens, N., Pascual, N., Fernández-Argüelles, M. T., Adrián, J., Costa-Fernández, J. M., Sánchez-Baeza, F., & Marco, M. P. (2011). Quantum dot-based array for sensitive detection of *Escherichia coli*. *Analytical and Bioanalytical Chemistry*, *399*(8), 2755-2762.

Scallan, E., Hoekstra, R. M., Angulo, F. J., Tauxe, R. V., Widdowson, M., Roy, S. L., Griffin, P. M. (2011). Foodborne illness acquired in the united States—major pathogens. *Emerg Infect Dis,* 17(1): 7-15

Scharff, R. L. (2012). Economic burden from health losses due to foodborne illness in the United States. *J. Food Prot.* 75(1): 123-131.

Seo, K., Brackett, R., Frank, J., & Hilliard, S. (1998). Immunomagnetic separation and flow cytometry for rapid detection of *Escherichia coli* O157: H7. *Journal of Food Protection,* 61(7), 812-816.

Shan, S., Zhong, Z., Lai, W., Xiong, Y., Cui, X., & Liu, D. (2014). Immunomagnetic nanobeads based on a streptavidin-biotin system for the highly efficient and specific separation of Listeria monocytogenes. *Food Control, 45,* 138-142.

Sharma, H., & Mutharasan, R. (2013). Review of biosensors for foodborne pathogens and toxins. *Sensors and Actuators B: Chemical,* 183, 535-549.

Shukla, S., Lee, G., Song, X., Park, S., & Kim, M. (2016). Immunoliposome-based immunomagnetic concentration and separation assay for rapid detection of *Cronobacter sakazakii*. *Biosensors and Bioelectronics,* 77, 986-994.

Song, Z., Hong, Y., Kwok, R. T., Lam, J. W., Liu, B., & Tang, B. Z. (2014). A dual-mode fluorescence "turn-on" biosensor based on an aggregation-induced emission luminogen. *Journal of Materials Chemistry B,* 2(12), 1717-1723.

STMicroelectronics, (2000). L298 datasheet. Geneva, Switzerlan.

Sung, Y. J., Suk, H. J., Sung, H. Y., Li, T., Poo, H., & Kim, M. G. (2013). Novel antibody/gold nanoparticle/magnetic nanoparticle nanocomposites for immunomagnetic separation and rapid colorimetric detection of Staphylococcus aureus in milk. *Biosensors and Bioelectronics, 43,* 432-439.

Tamanaha, C., Mulvaney, S., Rife, J., & Whitman, L. (2008). Magnetic labeling, detection, and system integration. *Biosensors and Bioelectronics,* 24(1), 1-13.

Texas Instruments, (1998). 74LS138 datasheet. Dallas, TX.

Turner, A., Karube, I., & Wilson, G. S. (1987). Biosensors: Fundamentals and Applications. Oxford, UK: Oxford University Press.

Valderrama, W. B., Dudley, E. G., Doores, S., & Cutter, C. N. (2016). Commercially available rapid methods for detection of selected food-borne pathogens. *Critical Reviews in Food Science and Nutrition,* 56(9), 1519-1531.

Velasco-Garcia, M. (2009). Optical biosensors for probing at the cellular level: A review of recent progress and future prospects. *Seminars in Cell & Developmental Biology,* 20(1) 27-33.

Velusamy, V., Arshak, K., Korostynska, O., Oliwa, K., & Adley, C. (2010). An overview of foodborne pathogen detection: In the perspective of biosensors. *Biotechnology Advances,* 28(2), 232-254.

Wang, B., Huang, X., Ma, M., Shi, Q., & Cai, Z. (2014). A simple quantum dot-based fluoroimmunoassay method for selective capturing and rapid detection of Salmonella Enteritidis on eggs. *Food Control, 35*(1), 26-32.

Wang, H., Li, Y., & Slavik, M. (2007). Rapid detection of Listeria monocytogenes using quantum dots and nanobeads-based optical biosensor. *Journal of Rapid Methods & Automation in Microbiology*, *15*(1), 67-76.

Wang, H., Li, Y., Wang, A., & Slavik, M. (2011). Rapid, sensitive, and simultaneous detection of three foodborne pathogens using magnetic nanobead–based immunoseparation and quantum dot–based multiplex immunoassay. *Journal of Food Protection,* 74(12), 2039-2047.

Wang, H., Li, Y., & Slavik, M. (2014). Rapid detection of Campylobacter jejuni in poultry products using quantum dots and nanobeads based fluorescent immunoassay. *International Journal of Poultry Science*, 13(5), 253.

Wang, L., Wu, C. S., Fan, X., & Mustapha, A. (2012). Detection of Escherichia coli O157: H7 and Salmonella in ground beef by a bead-free quantum dot-facilitated isolation method. *International Journal of Food Microbiology*, *156*(1), 83-87.

Wang, Y., Chen, Q., Gan, C., Yan, B., Han, Y., & Lin, J. (2016). A review on magnetophoretic immunoseparation. *Journal of Nanoscience and Nanotechnology,* 16(3), 2152-2163.

Xu, L., Callaway, Z. T., Wang, R., Wang, H., Slavik, M. F., Wang, A., & Li, Y. (2015). A fluorescent aptasensor coupled with nanobead-based immunomagnetic separation for simultaneous detection of four foodborne pathogenic bacteria. *Transactions of the ASABE*, 58(3), 891-906.

Xue, X., Pan, J., Xie, H., Wang, J., & Zhang, S. (2009). Fluorescence detection of total count of Escherichia coli and Staphylococcus aureus on water-soluble CdSe quantum dots coupled with bacteria. *Talanta*, *77*(5), 1808-1813.

Yang, L., & Li, Y. (2006). Simultaneous detection of *Escherichia coli* O157：H7 and *Salmonella* typhimurium using quantum dots as fluorescence labels. *Analyst,* 131(3), 394-401.

Yang, Y., Xu, F., Xu, H., Aguilar, Z. P., Niu, R., Yuan, Y., & Wan, C. (2013). Magnetic nano-beads based separation combined with propidium monoazide treatment and multiplex PCR assay for simultaneous detection of viable Salmonella Typhimurium, Escherichia coli O157: H7 and Listeria monocytogenes in food products. *Food Microbiology*, *34*(2), 418-424.

Yogeswaran, U., & Chen, S. (2008). A review on the electrochemical sensors and biosensors composed of nanowires as sensing material. *Sensors*, 8(1), 290-313.

Yu, J., Zhang, Y., Li, H., Yang, H., & Wei, H. (2016). Sensitive and rapid detection of *Staphylococcus aureus* in milk via cell binding domain of lysin. *Biosensors and Bioelectronics*, 77, 366-371.

Zhang, B., Wang, R., Wang, Y., & Li, Y. (2013). A portable impedance biosensor for detection of multiple avian influenza viruses. *Sensors*, 2013 IEEE, 1-4.

Zhang, X., Zhou, J., Zhang, C., Zhang, D., & Su, X. (2016). Rapid detection of *Enterobacter cloacae* by immunomagnetic separation and a colloidal gold-based immunochromatographic assay. *RSC Advances,* 6(2), 1279-1287.

Zhao, X., Lin, C., Wang, J., & Oh, D. H. (2014). Advances in rapid detection methods for foodborne pathogens. *J. Microbiol Biotechnol,* 24(3), 297-312.

Zhao, Y., Ye, M., Chao, Q., Jia, N., Ge, Y., & Shen, H. (2008). Simultaneous detection of multifood-borne pathogenic bacteria based on functionalized quantum dots coupled with immunomagnetic separation in food samples. *Journal of Agricultural and Food Chemistry*, 57(2), 517-524.

Zhu, H., Sikora, U., & Ozcan, A. (2012). Quantum dot enabled detection of *Escherichia coli* using a cell-phone. *Analyst*, 137(11), 2541-2544.